AGU PUBLICATIONS

Water Resources Research

RESEARCH ARTICLE
10.1002/2017WR021172

Snow Sublimation in Mountain Environments and Its Sensitivity to Forest Disturbance and Climate Warming

Graham A. Sexstone[1,2], David W. Clow[1], Steven R. Fassnacht[3,4,5], Glen E. Liston[4], Christopher A. Hiemstra[6], John F. Knowles[7,8], and Colin A. Penn[1]

[1]US Geological Survey, Colorado Water Science Center, Denver, CO, USA, [2]EASC-Watershed Science, Colorado State University, Fort Collins, CO, USA, [3]ESS-Watershed Science, Colorado State University, Fort Collins, CO, USA, [4]Cooperative Institute for Research in the Atmosphere, Fort Collins, CO, USA, [5]Geospatial Centroid at CSU, Fort Collins, CO, USA, [6]U.S. Army Cold Regions Research and Engineering Laboratory, Fort Wainwright, AK, USA, [7]Institute of Arctic and Alpine Research, University of Colorado Boulder, Boulder, CO, USA, [8]School of Geography and Development, University of Arizona, Tucson, AZ, USA

Key Points:
- Sublimation losses to the atmosphere were equivalent to 28% of winter precipitation and were relatively greater during low snow years
- Forested areas accounted for the majority of sublimation and bark-beetle disturbance reduced this flux by 4%
- The net sublimation flux decreased under warming climate scenarios due to reductions in snow covered area and duration

Supporting Information:
- Supporting Information S1

Correspondence to:
G. Sexstone,
sexstone@usgs.gov

Citation:
Sexstone, G. A., Clow, D. W., Fassnacht, S. R., Liston, G. E., Hiemstra, C. A., Knowles, J. F., & Penn, C. A. (2018). Snow sublimation in mountain environments and its sensitivity to forest disturbance and climate warming. *Water Resources Research*, *54*, 1191–1211. https://doi.org/10.1002/2017WR021172

Received 24 MAY 2017
Accepted 30 JAN 2018
Accepted article online 6 FEB 2018
Published online 23 FEB 2018

Abstract Snow sublimation is an important component of the snow mass balance, but the spatial and temporal variability of this process is not well understood in mountain environments. This study combines a process-based snow model (SnowModel) with eddy covariance (EC) measurements to investigate (1) the spatio-temporal variability of simulated snow sublimation with respect to station observations, (2) the contribution of snow sublimation to the ablation of the snowpack, and (3) the sensitivity and response of snow sublimation to bark beetle-induced forest mortality and climate warming across the north-central Colorado Rocky Mountains. EC-based observations of snow sublimation compared well with simulated snow sublimation at stations dominated by surface and canopy sublimation, but blowing snow sublimation in alpine areas was not well captured by the EC instrumentation. Water balance calculations provided an important validation of simulated sublimation at the watershed scale. Simulated snow sublimation across the study area was equivalent to 28% of winter precipitation on average, and the highest relative snow sublimation fluxes occurred during the lowest snow years. Snow sublimation from forested areas accounted for the majority of sublimation fluxes, highlighting the importance of canopy and sub-canopy surface sublimation in this region. Simulations incorporating the effects of tree mortality due to bark-beetle disturbance resulted in a 4% reduction in snow sublimation from forested areas. Snow sublimation rates corresponding to climate warming simulations remained unchanged or slightly increased, but total sublimation losses decreased by up to 6% because of a reduction in snow covered area and duration.

1. Introduction

In mountainous and cold regions of the world, snow water equivalent (SWE) stored in seasonal snowpacks provides a critical water resource for ecological and human needs. In the simplest terms, the melted water from snow that is available for subsurface recharge, vegetation uptake, and runoff to streams each year can be described as total winter precipitation minus net snow sublimation (Liston & Sturm, 2004), where snow sublimation is defined as the transfer of water directly between snow and the atmosphere through phase change. However, this basic mass balance is challenging to evaluate due to variability in seasonal snow cover over space and time that results from wind-induced snow transport and its interactions with topography and forest canopy features (e.g., Elder et al., 1991). Additionally, there is considerable uncertainty in measuring both precipitation (e.g., Goodison et al., 1998) and snow sublimation (e.g., Sexstone et al., 2016), and reliable winter observations of these variables in seasonally snow-covered areas are sparse (Bales et al., 2006). In arid and semi-arid regions, previous work suggests that snow sublimation represents an important component of the snow mass balance (Cline, 1997; Gustafson et al., 2010; Hood et al., 1999; Kattelmann & Elder, 1991; Knowles et al., 2015; Marks & Dozier, 1992; Marks et al., 2008; Meiman & Grant, 1974; Molotch et al., 2007; Montesi et al., 2004; Reba et al., 2012; Sexstone et al., 2016). However, many of these investigations were based on point measurements, and few studies have rigorously evaluated the spatial and temporal variability of snow sublimation within complex mountainous terrain (e.g., Gascoin et al., 2013; MacDonald et al., 2010; Strasser et al., 2008). Given the importance of seasonal snow cover to water

resources, there is a need to better understand the spatio-temporal contribution of snow sublimation to the annual water balance in mountainous regions.

Snow sublimation, hereafter referred to as sublimation, encompasses water vapor fluxes between the atmosphere and the snowpack surface (surface sublimation), intercepted snow held within the forest canopy (canopy sublimation), and snow that is transported by wind (blowing snow sublimation). The key mechanisms that drive sublimation flux are the (1) available energy for turbulent flux, (2) vapor pressure gradient between the snow and atmosphere, and (3) wind speed and exposure (e.g., Sexstone et al., 2016). Previous studies have reported that surface sublimation in mountainous areas is equivalent to 10–20% of winter precipitation in open areas (Hood et al., 1999; Kattelmann & Elder, 1991; Marks & Dozier, 1992; Reba et al., 2012; Sexstone et al., 2016) and less than 10% of winter precipitation in sheltered and sub-canopy areas (Marks et al., 2008; Reba et al., 2012). Canopy sublimation across various coniferous forest types has been reported on the order of 30–40% of annual snowfall (Pomeroy & Gray, 1995). In the Colorado Rocky Mountains, canopy sublimation measured by Montesi et al. (2004) accounted for 20–30% of total snowfall. Estimations of blowing snow sublimation from different environments vary greatly, but can represent a significant loss term in the snow mass balance, ranging between 10 and 50% of seasonal snowfall (Pomeroy & Essery, 1999; Pomeroy & Gray, 1995). However, other studies have suggested that temperature and humidity feedbacks during blowing snow sublimation events limit this process (Dery et al., 1998; Groot Zwaaftink et al., 2013). Since the spatial variability and relative importance of sublimation in mountainous environments is based on how the driving mechanisms of sublimation interact with variations of land cover and topography (e.g., Strasser et al., 2008), process-based snow modeling systems that can simulate snowpack processes over space and time (e.g., Lehning et al., 2006; Liston & Elder, 2006b; Pomeroy et al., 2007) can constrain the role of sublimation across various snow and climate regimes that rely on snowmelt as an important water resource.

Many studies have investigated the response of snowpack dynamics to forest disturbances and changing climate conditions, but potential changes to sublimation from these perturbations are not well understood. For example, seasonally snow-covered forests in western North America have experienced substantial disturbance from mountain pine beetle (*Dendroctonus ponderosae*) and spruce beetle (*Dendroctonus rufipennis*) outbreaks (Potter & Conkling, 2016), which have resulted in widespread tree mortality and thus changes to forest structure that are particularly relevant to canopy and surface sublimation processes. Field studies that have focused on measuring SWE in both un-impacted and disturbed forests have inferred decreasing (e.g., Boon, 2012; Pugh & Small, 2012) as well as steady or increasing (e.g., Biederman et al., 2014; Harpold et al., 2014) net sublimation fluxes in the presence of disturbance. In contrast, distributed watershed modeling studies considering beetle-induced forest mortality (e.g., Livneh et al., 2015; Penn et al., 2016) have generally reported decreased evapotranspiration, but have not specifically focused on the sublimation component of evapotranspiration. Although changes to snow accumulation and melt processes from climate warming have been studied widely (e.g., Clow, 2010; Harpold et al., 2012; Knowles et al., 2006; McCabe & Wolock, 2007; Mote, 2006; Musselman et al., 2017; Rauscher et al., 2008; Stewart, 2009), the response of sublimation to climate change has received little investigation. As a result, specific knowledge gaps remain including how the components of sublimation will individually and collectively respond to changes in forcing mechanisms, in addition to changing snow accumulation and melt dynamics. Process-based snow models that can integrate responses and feedbacks of the snow energy balance offer the ability to evaluate sublimation responses to these changing land cover and climate conditions, which is critically important to predictive understanding of the water balance in snow-dominated regions.

In this study, we used SnowModel (Liston & Elder, 2006b), a well-validated process-based snow modeling system, to simulate snowpack processes for five water years (WY) (i.e., 1 October to 30 September) over a model domain that spanned 3,600 km^2 in north-central Colorado, United States (U.S.). Model simulations allowed for annual quantification of the parsed surface, canopy, and blowing snow sublimation fluxes across the study domain. The specific objectives of this study were to (1) compare and contrast the spatio-temporal variability of simulated and measured (via the eddy covariance method) sublimation across the domain, (2) quantify the contribution of simulated surface, canopy, and blowing snow sublimation fluxes to the seasonal ablation of the snowpack, and (3) assess the sensitivity and response of simulated sublimation to both forest disturbance and climate warming scenarios.

2. Methodology

2.1. Study Area

The study area was a 40 km × 90 km domain that ranged in elevation from 2,261 m to 4,345 m (mean elevation of 3,059 m) above sea level (Figure 1). Approximately 22% of this area was located above treeline (i.e., bare rock and alpine tundra), 58% was forested (99% coniferous forest, 1% deciduous forest, and 0.02% mixed forest), and 20% was nonforested below treeline (i.e., grasslands, wetlands, shrublands, open water, and developed) (accessed: <http://www.mrlc.gov/nlcd2011.php>). In general, the lowest elevations were characterized by gently sloping topographic features compared to the highest elevations, which exhibited steep and complex topography. The study domain included the headwaters of the Upper Colorado, North Platte, and South Platte River Basins and was dominantly composed of federal lands, including Rocky Mountain National Park and the Arapaho and Roosevelt National Forests and associated Wildernesses; the North American Continental Divide intersected the study domain from north to south. Continental snowpacks are typical of mountains in this area (Trujillo & Molotch, 2014), which can be characterized by persistent, transitional, or intermittent snow-cover zones (Richer et al., 2013), and generally exhibit peak snow accumulation during the springtime months of April and May.

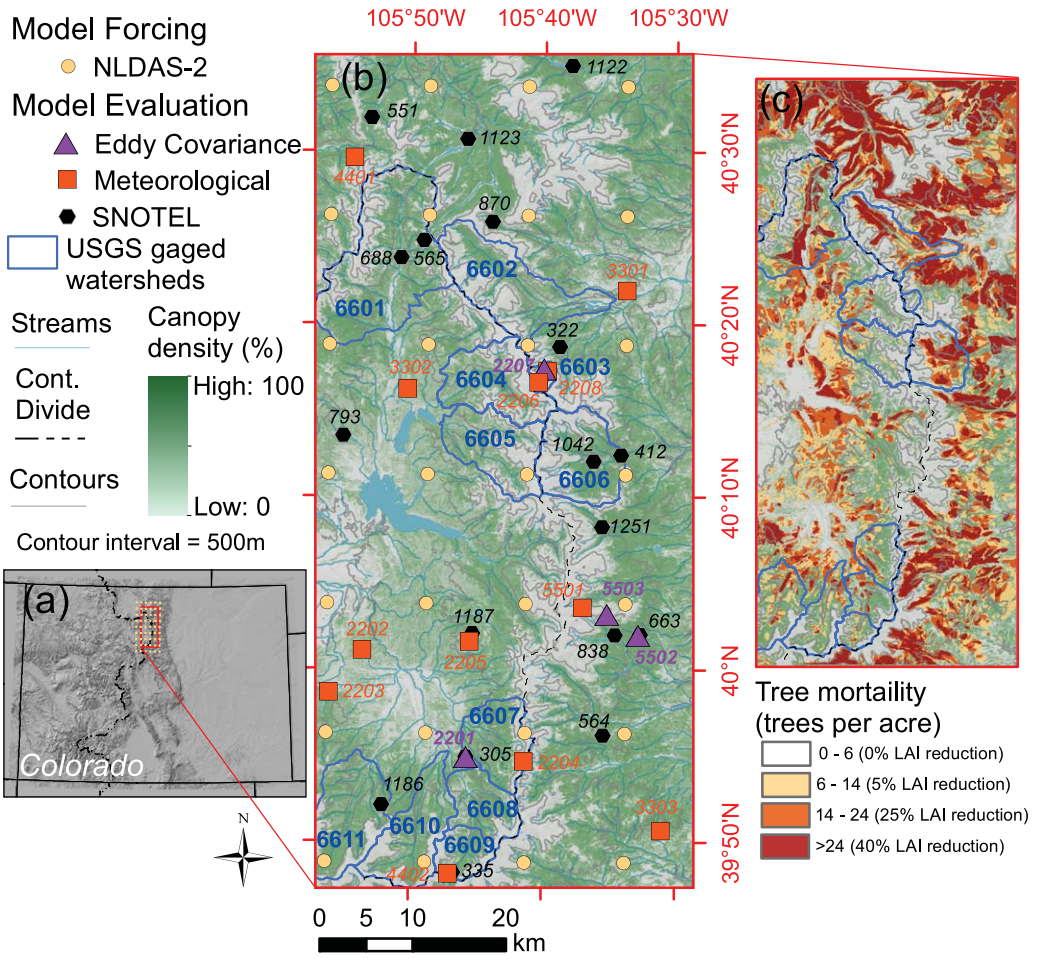

Figure 1. Study area map showing the (a) study domain location within the north-central Colorado Rocky Mountains, U.S., (b) canopy density (Homer et al., 2015) with 500 m elevation contours and all model evaluation station locations highlighted and labeled by station ID (identified in supporting information Table S1) and North American Land Data Assimilation System (NLDAS-2) locations highlighted, and (c) tree mortality (1997–2015) and associated leaf area index (*LAI*) reduction based on USDA Forest Service Insect and Disease Detection Surveys (accessed: <http://foresthealth.fs.usda.gov/portal/Flex/IDS>).

2.2. Model Description

SnowModel is a spatially distributed snow evolution modeling system specifically designed to apply to a wide range of topography, land cover, and climate conditions where precipitation falls as snow (Liston & Elder, 2006b). SnowModel has been rigorously validated in seasonally snow-covered forested and alpine environments similar to the study area (e.g., Greene et al., 1999; Hiemstra et al., 2006; Liston & Elder, 2006a, 2006b; Liston et al., 2008; Prasad et al., 2001; Sproles et al., 2013). SnowModel includes four sub-models: MicroMet (Liston & Elder, 2006a), which is a meteorological distribution model; EnBal (Liston, 1995), which calculates surface energy exchanges between the snow and atmosphere; SnowPack (Liston & Hall, 1995), which simulates the seasonal evolution of snowpack properties; and SnowTran-3D (Liston & Sturm, 1998; Liston et al., 2007), which accounts for snow redistribution by wind. Spatially varying fields of elevation and land cover and temporally varying meteorological forcing data are required to run SnowModel, in order to simulate the spatial distribution and seasonal evolution of snow using the first-order physics described in the sub-models above. SnowModel's ability to represent sublimation is critical to accurate simulation of the spatial distribution of SWE in complex mountainous environments. In addition to surface sublimation from the snowpack, SnowModel also simulates blowing snow sublimation processes that are particularly important in alpine tundra environments, as well as canopy interception and subsequent sublimation processes that are unique to forested environments. The equations used for calculating each component of sublimation in SnowModel are described in the supporting information (Hedstrom & Pomeroy, 1998; Liston, 1995; Liston & Elder, 2006b; Liston & Sturm, 1998; Louis, 1979; Mahat & Tarboton, 2014; Oke, 1987; Pomeroy et al.,1998; Price & Dunne, 1976).

2.3. Model Simulations

2.3.1. Baseline Simulations

SnowModel was run at an hourly time step for the entire model domain (Figure 1) at a grid resolution of 100 m from WY 2011 through WY 2015. These simulations are hereafter referred to as baseline simulations. The spatially varying fields of elevation, land cover, and canopy cover fraction used for all simulations were provided by the U.S. Geological Survey (USGS) national elevation data set and national land cover database spatial data sets (30 m grid resolution) (accessed: <http://ned.usgs.gov> and <http://www.mrlc.gov/nlcd2011.php>, respectively) and were resampled to a 100 m grid resolution. The land cover data set was reclassified based on the pre-defined vegetation types defined by SnowModel (refer to Liston & Elder, 2006b). Effective leaf area index (*LAI**) values across the domain were created by scaling the maximum *LAI** for each forest class vegetation type (Table 1) by the fraction of canopy coverage (i.e., 100% canopy coverage equals the maximum *LAI**) for each 100 m grid as described by Broxton et al. (2015).

Hourly air temperature, precipitation, relative humidity, and wind speed and direction meteorological forcing data were provided by the 1/8th-degree grid spacing North American Land Data Assimilation System (NLDAS-2) reanalysis forcing data set (accessed: https://ldas.gsfc.nasa.gov/nldas/; (Mitchell et al., 2004)) (Figure 1). The mean elevation of each NLDAS-2 grid cell was used by the MicroMet sub-model to downscale the meteorological forcing to a 100 m spatial resolution for the model simulations (e.g., Liston & Elder, 2006a; Liston & Hiemstra, 2011; Liston et al., 2008) based on northern hemisphere monthly lapse rates (refer to Liston & Elder, 2006a) and the 100 m digital elevation model. Additionally, an observed negative bias in the NLDAS-2 precipitation forcing data was adjusted for each of the baseline simulations using a linear scaling of the precipitation forcing that ranged between 10 and 24% (supporting infomation Table S2). The NLDAS-2 precipitation forcing adjustment for each year of the baseline simulations was determined based on a mean comparison between the MicroMet downscaled NLDAS-2 precipitation forcing and measured SNOTEL (SNOpack TELemetry) precipitation within the study area (Figure 1 and supporting infomation Table S2).

Table 1
Forest Class Descriptions and Associated Winter and Summer Maximum LAI* *Values*

Forest class description	Example forest type	Maximum *LAI** (winter/summer)
Coniferous forest	Spruce-fir, lodgepole pine, ponderosa pine	4.0/4.0
Deciduous forest	Aspen	0.5/2.5
Mixed forest	Aspen spruce-fir lodgepole pine mixed	2.3/3.3

Note. Maximum *LAI** values were derived from observed literature values within the study domain (Liston & Elder, 2006b; Turnipseed et al., 2002).

2.3.2. Sensitivity Simulations

In addition to the baseline SnowModel simulations, two model experiments were completed to assess the sensitivity of simulated sublimation to scenarios representing changing land cover and climate. The first model experiment evaluated the sensitivity of sublimation to insect-related tree mortality that has been widespread within the study domain (Bright et al., 2013). The USDA Forest Service Insect and Disease Detection Survey spatial data sets (accessed:

<http://foresthealth.fs.usda.gov/portal/Flex/IDS>) from 1997 through 2015 were compiled to quantify tree mortality during the modeled time period within the study domain (Figure 1). The distribution of tree mortality within the study domain was divided into four quantiles representing no mortality, light mortality, moderate mortality, and severe mortality (Bright et al., 2013; Figure 1). These quantiles were used to reduce the spatially variable *LAI** across the study domain by 0%, 5%, 25%, and 40%, respectively (Bright et al., 2013; Pugh & Gordon, 2013). A total of 29% of forested area within the study domain was classified as light to severe mortality (10% light mortality, 8% moderate mortality, 11% severe mortality). Reductions to *LAI** were ingested into SnowModel to represent forest cover changes due to insect-induced tree mortality during WY 2011 through WY 2015, and these results were subsequently compared to the baseline simulations.

The second model experiment was designed to evaluate the sensitivity of SnowModel simulated sublimation to future climate conditions predicted by general circulation models (GCMs) that were dynamically downscaled using a regional climate model, RegCM3 (Hostetler et al., 2011). The RegCM3 regional climate model simulations, described in detail by Hostetler et al. (2011), were derived for present and future climate scenarios over western North America (15 km resolution) using output from four GCMs to simulate boundary conditions. Trace gas concentrations for all RegCM3 and GCM simulations were based on the 20th century and A2 scenarios developed for the Intergovernmental Panel on Climate Change (IPCC) AR4 report (Solomon et al., 2007). The A2 scenario is similar to the representative concentration pathway (RCP) 8.5 scenario developed for the IPCC AR5 report (Hostetler et al., 2011; Stocker et al., 2013). This study used the ensemble of RegCM3 GCM simulations (accessed: <https://cida.usgs.gov/gdp/>) to compute area-weighted mean monthly air temperature, precipitation, relative humidity, and wind speed across the SnowModel domain for three 20 year periods of time: the historic period (1980–1999), future period S1 (2016–2035) (supporting infomation Figure S1), and future period S2 (2046–2065) (supporting infomation Figure S2). The monthly differences between the S1 and S2 periods and the historic period were computed for each forcing variable (Table 2), and were subsequently used to adjust the SnowModel meteorological forcing data from each of the baseline simulations. Therefore, for WY 2011 through WY 2015, three model simulations (baseline, S1 (2016–2035), and S2 (2046–2065)) were evaluated to assess the sensitivity of sublimation to future warming climate conditions. During the winter (October–May), the mean perturbations to climate prescribed by this study were increased air temperature of 0.6°C and 1.7°C, increased precipitation of 1.5% and 2.3%, decreased relative humidity of −0.3% and −1.0%, and decreased wind speed of −0.1 m s^{-1} and −0.1 m s^{-1} in the S1 and S2 scenarios, respectively (Table 2).

Table 2
Month-Varying Perturbations Applied to Air Temperature, Precipitation, Relative Humidity, and Wind Speed Meteorological Forcing Data for the S1 (2016–2035) and S2 (2046–2065) SnowModel Climate Sensitivity Simulations

	Air temperature (°C)		Precipitation (% change)		Relative humidity (%)		Wind speed (m s^{-1})	
Month	S1	S2	S1	S2	S1	S2	S1	S2
10	1.1	2.2	−9.7	−1.2	−0.8	−1.6	−0.2	−0.1
11	1.2	2.3	14.3	4.5	−0.6	−1.6	−0.2	−0.4
12	0.6	1.9	−1.5	4.1	−1.1	−1.3	−0.9	−0.3
1	0.4	1.4	0.8	16.1	0.2	0.3	0.4	0.0
2	0.8	1.0	5.1	0.6	0.2	−0.3	−0.3	−0.6
3	0.5	1.5	0.4	10.3	−0.4	−0.5	0.2	0.6
4	0.1	1.5	4.5	−2.3	0.1	−1.2	−0.3	0.2
5	0.3	1.9	−1.7	−13.6	0.4	−1.7	0.4	0.2
6	0.6	2.4	3.4	7.5	−1.0	−2.7	0.0	−0.3
7	0.7	2.5	−9.0	−15.2	−2.7	−4.4	0.1	0.2
8	0.8	2.4	−14.4	−9.0	−3.1	−3.7	0.3	0.0
9	0.5	2.1	−4.7	−3.8	−0.6	−0.6	0.4	0.4
Mean	0.6	1.9	−1.0	−0.2	−0.8	−1.6	0.0	0.0
Std dev	0.3	0.5	7.7	9.4	1.1	1.4	0.4	0.3

2.4. Model Evaluation

2.4.1. Meteorological and Snow Observations

Daily mean observations from 34 meteorological stations within the model domain were used to evaluate the meteorological forcing and snowpack evolution of the baseline model simulations (Figure 1 and supporting infomation Table S1). SNOTEL stations (n = 18) were also used to adjust the mean bias of the NLDAS-2 precipitation forcing (supporting infomation Table S2). Model evaluation performance statistics were computed based on daily values using the coefficient of determination (R^2), mean bias (*Bias*) for daily variables, percent bias (*PBias*) for cumulative variables, and root mean squared error (*RMSE*). SNOTEL stations were used to evaluate the performance of the precipitation forcing magnitude and variability. Additionally, other meteorological stations within the study area (n = 16) were used to evaluate meteorological forcing due to air temperature, relative humidity, and wind speed. Daily observations of SWE at SNOTEL stations were used to assess the performance of the simulated snow mass balance; values equal to zero were not included in this analysis. Given that SWE measurements at SNOTEL stations are generally located in small sheltered forest openings, simulated SWE was assumed not to be influenced by forest canopy interception or wind redistribution processes. Land cover grids (100 m) that overlapped SNOTEL station locations were classified as grassland vegetation type, and snow redistribution by wind was not simulated for these specific grid cells. Additionally, daily observations of snow depth at other meteorological stations (n = 6) were used to constrain simulated snow depth evolution, and were not evaluated when observed or simulated values were equal to zero. These stations were generally located in exposed locations that were useful for evaluating the model's ability to simulate snow depth in areas characterized by persistent wind redistribution of snow. Lastly, simulated snow cover duration was evaluated using remotely sensed Moderate Resolution Imaging Spectroradiometer (MODIS) snow covered area (SCA) data from the MOD10A2 product (accessed: <https://nsidc.org/data/mod10a2>). Model grid cells were flagged as snow-covered if the simulated SWE was greater than 10 mm on the same day (Gascoin et al., 2013). The maximum snow cover extent across the model domain (observed by MODIS for every 8 day period) was compared to the maximum snow cover extent simulated by SnowModel during the same period. The 8 day MODIS SCA product was used in favor of the daily MODIS SCA product in order to minimize the influence of cloud coverage on the model evaluation of snow cover duration.

2.4.2. Sublimation Observations

Surface-atmosphere water vapor fluxes were measured directly using the eddy covariance (EC) method during snow-covered periods, and were used to quantify sublimation at four stations within the model domain (purple triangles in Figure 1). Sublimation has been quantified using the EC method by many studies (e.g., Helgason & Pomeroy, 2012; Knowles et al., 2012; Marks et al., 2008; Molotch et al., 2007; Pomeroy & Essery, 1999; Reba et al., 2012; Sexstone et al., 2016); Sexstone et al. (2016) discussed the relative merits and limitations of this method for monitoring surface sublimation. EC measurements were made at the Arrow (grassland forest opening), Andrews Meadow (subalpine meadow), US-NR1 AmeriFlux (subalpine forest), and T-Van (alpine tundra) stations (Figure 1 and supporting infomation Table S1). The Arrow station (2,955 m) is located within a moderately sloping (20%; 290° aspect), large (~ 600 m) grassland opening of surrounding lodgepole pine (*Pinus contorta*) forest. The Andrews Meadow station (3,205 m) is located in a small (~ 200 m) subalpine wetland meadow within the Loch Vale watershed, Rocky Mountain National Park. Measurements collected by EC were made at the Arrow and Andrews Meadow stations during the snow-covered periods of WY 2014 and WY 2015. The US-NR1 station (3,050 m) is positioned within subalpine forest primarily composed of subalpine fir (*Abies lasiocarpa*), Engelmann spruce (*Picea engelmannii*), and lodgepole pine with EC instrumentation located approximately 10 m above the top of the forest canopy. The T-Van station (3,503 m) is located on a gently sloping (8%) alpine tundra meadow. Both the US-NR1 and T-Van stations are contained within the Niwot Ridge Long Term Ecological Research (LTER) Program study area, and EC measurements at these stations were collected during October 2011 through December 2014 of the study period. Water vapor fluxes were calculated at each station from the covariance between fluctuations of the vertical wind speed and water vapor density. Post processing of the EC water vapor fluxes consisted of standard EC corrections, data screening, and gap-filling (e.g., Reba et al., 2009). A description of the specific post-processing methods used for the Arrow and Andrews Meadow stations is described in Sexstone et al. (2016), and details for post processing of the US-NR1 and T-Van fluxes can be found in Burns et al. (2014) and Knowles et al. (2012), respectively.

The simulated cumulative snow season and daily sublimation were compared to water vapor fluxes measured at the four EC stations within the model domain. Simulated sublimation at each observation station

was averaged among the grid cells that were 400 m in the upwind direction from each station to represent the typical statistical measurement (flux) footprint at these stations. Although flux footprints can be variable over space and time (Sogachev et al., 2004), this work did not investigate the implications of selecting different footprint sizes for model evaluation following Svoma (2017) who determined that simulated sublimation was insensitive to footprint size for a similar analysis. The evaluation of simulated sublimation at the Arrow, Andrews Meadow, US-NR1 and T-Van stations included a comparison of simulated surface, canopy, and blowing snow sublimation to the observed EC sublimation flux.

2.4.3. Water Balance

To evaluate simulated sublimation fluxes at the watershed scale, water balance calculations were computed for 11 USGS-gaged watersheds within the model domain (Figure 1 and supporting infomation Table S1) during the snow accumulation and melt period (1 October to 31 July) of each simulation year using the water balance equation:

$$\text{Runoff} = \text{precipitation} - \text{sublimation} \pm \text{blowing snow transport} - \text{evapotranspiration}. \quad (1)$$

Observed runoff was calculated from stream-gage records for each watershed (USGS National Water Information System: <http://doi.org/10.5066/F7P55KJN>). Precipitation, sublimation, and blowing snow transport were derived from spatially distributed SnowModel output and totaled for each watershed during the snow accumulation and melt period. Since SnowModel does not simulate evapotranspiration (*ET*), *ET* was estimated for each watershed using output from the MODIS-based Simplified Surface Energy Balance (SSEBop) model (Senay et al., 2013). Area-weighted monthly mean SSEBop *ET* estimates for each watershed from April through July of each water year were used to quantify growing season *ET* (accessed: <https://cida.usgs.gov/gdp/>). Changes in watershed storage were not estimated in the water balance evaluation, thus storage is an unresolved loss not included in equation (1). To characterize uncertainty in the water balance, uncertainty associated with individual water balance components was estimated and summed. The uncertainty in both simulated cumulative precipitation and simulated sublimation was calculated based on the mean of absolute values of percent bias calculations from each year. The uncertainties for blowing snow transport, *ET*, and runoff were estimated to be 25%, 25% (Senay et al., 2013), and 10%, respectively for each year. Uncertainties in the individual water balance components were combined using the standard error propagation formula (e.g., Knowles et al., 2015; Sexstone et al., 2016; Taylor, 1997).

3. Results and Discussion

3.1. Model Evaluation

The MicroMet sub-model provided a well-simulated representation of the meteorological conditions across the study area during each of the baseline simulations (Table 3). The daily mean simulated air temperature was linearly related with daily mean observations, with R^2 values ranging from 0.89 to 0.98 (all p-values < 0.01; supporting infomation Table S3) and a mean bias of -0.4°C amongst all stations and years (supporting infomation Table S3). Simulated relative humidity was also significantly related (mean $R^2 = 0.68$; all p-values < 0.01) to daily mean meteorological observations (supporting infomation Table S4), but was consistently biased low (mean bias = -5%; Table 3), which could contribute to an overestimation of simulated snow sublimation. Simulated wind speeds were modestly related with daily wind speed observations (mean $R^2 = 0.48$; all p-values < 0.01), and were biased high at low elevation stations and biased low at high elevation stations across the domain. The overall mean wind speed bias of -0.2 m s^{-1} could affect simulated snow sublimation based on elevation (Table 3 and supporting infomation Table S5). Simulated and observed cumulative precipitation were highly linearly related (mean $R^2 = 0.99$; all p-values < 0.01); simulated precipitation was biased slightly high with a mean *PBias* of 8% and *RMSE* of 59 mm (Table 3 and supporting infomation Table S6).

Simulated and observed SWE were highly linearly related (mean $R^2 = 0.86$; all p-values < 0.01), but the simulated SWE overestimated (mean *PBias* = 5%) daily mean SWE measurements at SNOTEL stations

Table 3
Mean Summary Values of Annual Station Performance Statistics for Each of the Model Evaluation Variables

Variable	Number stations	R^2	*Bias*	*RMSE*
Air temperature (°C)	16	0.95	−0.4	2.0
Relative humidity (%)	16	0.68	−5	13
Wind speed (m s^{-1})	15	0.48	−0.2	3.0
Cumulative precipitation (mm)	17	0.99	@8%	59
Snow water equivalent (mm)	18	0.86	@5%	71
Snow depth (m)	6	0.75	@-9%	0.31
Snow covered area (fraction)	n/a	0.87	0.06	0.14
Cumulative sublimation (mm)	4	0.92	@67%	62
Cumulative sublimation[a] (mm)	4	0.97	@-4%	20
Sublimation rate (mm/d)	4	0.14	0.24	1.6
Sublimation rate[a] (mm/d)	4	0.19	−0.11	0.8

Note. See supporting information Tables S3 through S13 for model evaluation statistics for individual stations and water years.

[a]Simulated snow sublimation excluding the simulated blowing snow sublimation component. Summary values of mean bias are provided for all variables unless denoted by @, which indicates percent bias was computed.

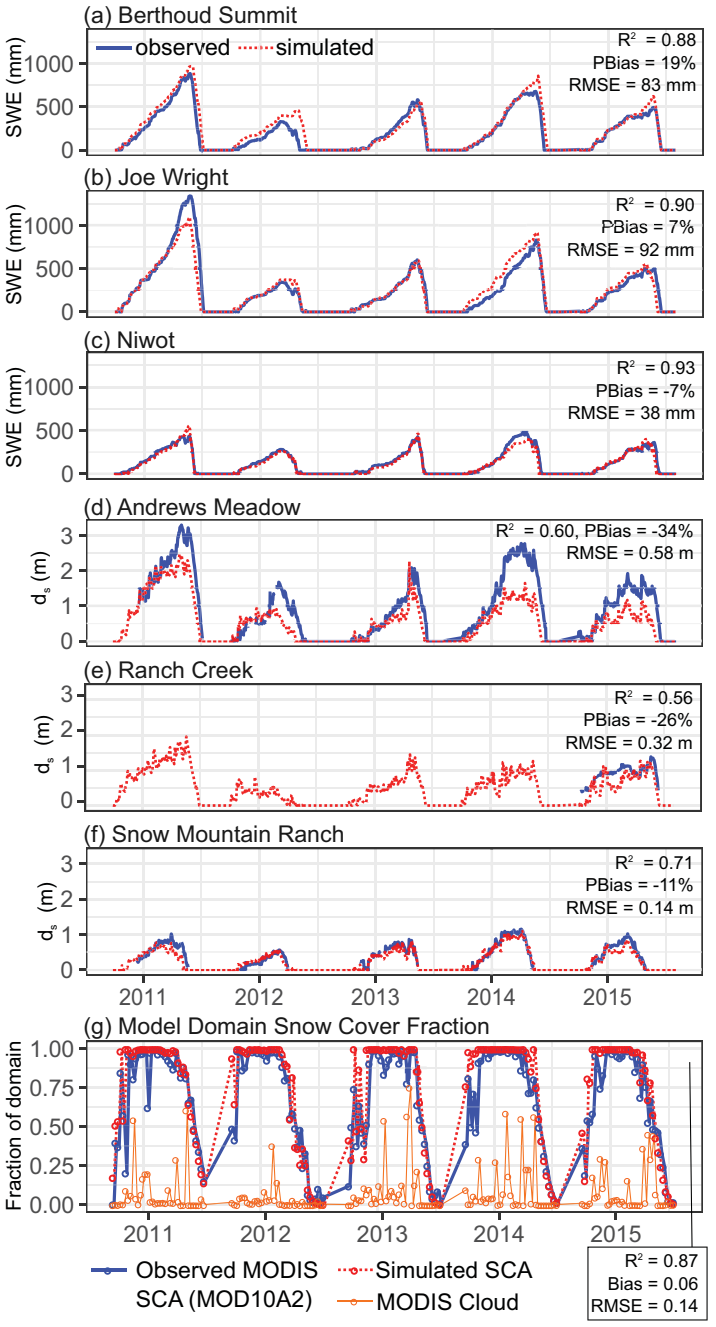

Figure 2. Time series plots and model evaluation statistics of daily observed SNOTEL snow water equivalent (SWE) compared to daily simulated SWE at the (a) Berthoud Summit, (b) Joe Wright, and (c) Niwot SNOTEL stations; daily observed snow depth (d_s) compared to daily simulated d_s at the (d) Andrews Meadow, (e) Ranch Creek, and (f) Snow Mountain Ranch stations; and (g) observed MODIS 8 day maximum snow cover extent compared to simulated 8 day maximum snow cover extent across the model domain.

(Table 3 and supporting infomation Table S7). Errors in simulated SWE were most related to errors in simulated precipitation amount and/or springtime precipitation phase (Figure 2). Simulated SWE errors may be attributed to differences in precipitation gage undercatch among precipitation observations used to adjust the precipitation forcing data set (e.g., Fassnacht, 2004; Goodison et al., 1998; Meyer et al., 2012) or the scale difference between the model grid and SNOTEL snow pillow measurements (Kashipazha, 2012; Meromy et al., 2013).

The relation between simulated and observed snow depth was variable on an inter-annual basis (supporting infomation Table S8) (mean $R^2 = 0.75$). Simulated snow depth generally underestimated (mean $PBias = -9\%$) snow depth measurements at measurement stations (Table 3) located in open areas that were useful for evaluating simulated blowing snow processes (e.g., transport and sublimation). Figure 2 compares simulated and observed snow depth at three of the snow depth measurement stations that experienced varying degrees of blowing snow redistribution (based on field observations). The largest errors in simulated snow depth occurred at the Andrews Meadow station (Figure 2d), which was characterized by moderate blowing snow redistribution. Errors in simulated snow depth may thus be influenced by an overestimation of simulated wind redistribution at this station, or by errors in simulated precipitation as shown by nearby SNOTEL stations (supporting infomation Table S6). Simulated snow depth compared favorably to observations at the Ranch Creek station (Figure 2e), which was located in an alpine environment with substantial amounts of blowing snow redistribution, and at the lower-elevation (minimal blowing snow redistribution) Snow Mountain Ranch station (Figure 2f). Domain-wide simulated snow cover duration was significantly related to remotely sensed MODIS SCA remotely sensed observations (R^2 ranging from 0.75 to 0.93; all p-values < 0.01; supporting infomation Table S9), particularly during the snowmelt period (Figure 2g). The mean bias of the simulated domain snow cover fraction showed a slightly positive bias that ranged from 0.04 to 0.08. These results indicate that the baseline SnowModel simulations reasonably represented important snow accumulation, redistribution, duration, and melt processes.

Simulated cumulative sublimation from stations located in forest openings (Arrow, Andrews Meadow) and alpine tundra (T-Van) were biased high compared to EC observations (Figure 3). EC observations at these stations were similar in both magnitude and temporal evolution to simulated cumulative sublimation excluding simulated blowing snow sublimation (Table 3; supporting information Tables S10 and S11). In contrast, simulated cumulative sublimation estimates from the forested station (US-NR1) compared favorably with EC observations (mean $PBias = -0.4\%$; supporting infomation Table S10). Overall, daily simulated sublimation rates and daily observed EC sublimation rates exhibited considerable scatter around the one-to-one line and similar correlation and bias to the comparison of simulated and observed cumulative sublimation (Figure 4).

The evaluation of simulated versus observed sublimation at the US-NR1 station included a combination of canopy and sub-canopy sublimation processes that occur in forested areas. Although EC observations from below the canopy at US-NR1 were not available during the study period, Molotch et al. (2007) used EC observations from 1 March through 10 April 2002 to contrast sub-canopy surface (0.41 mm d^{-1}) and canopy (0.71 mm d^{-1}) sublimation rates at this site. For comparison, the mean simulated sub-canopy surface

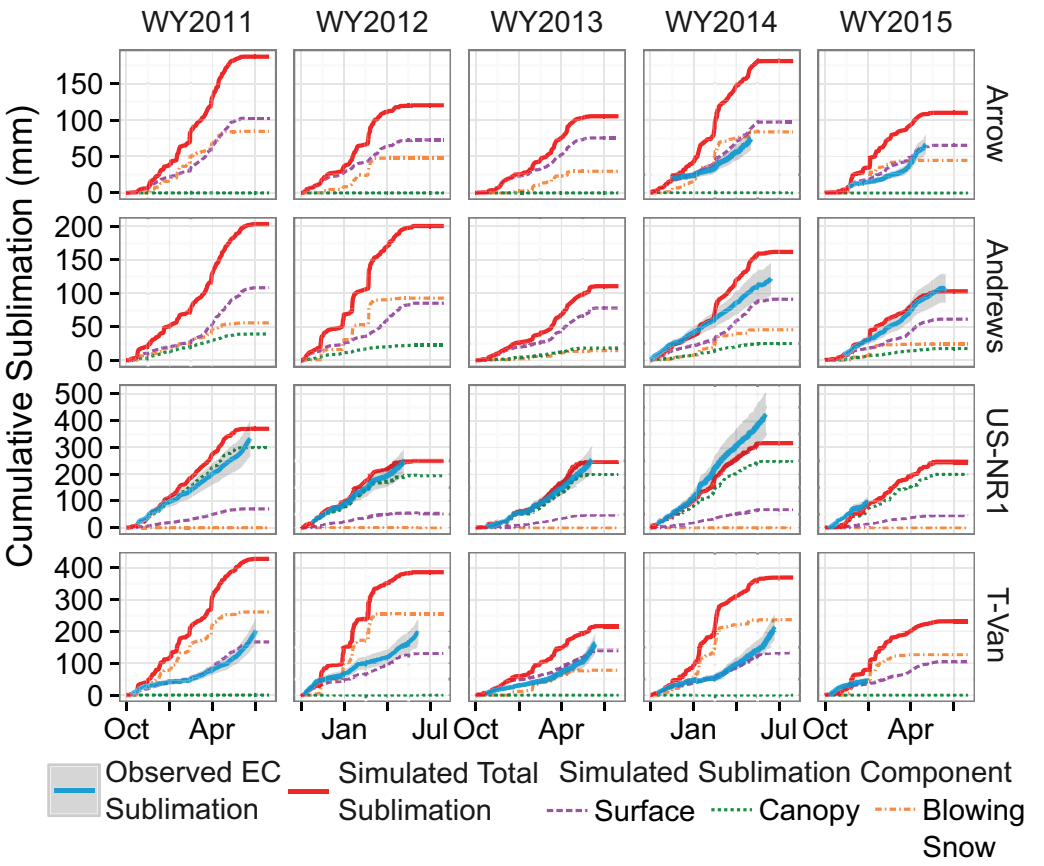

Figure 3. Time series plots of the daily observed eddy covariance (EC) cumulative sublimation flux (blue line) and associated measurement uncertainty (gray shading) (±20%; Andreas et al., 2010) compared to the daily simulated sublimation flux (red line) and individual sublimation components (surface sublimation, purple dashed line; canopy sublimation, green dotted line; blowing snow sublimation; orange dashed-dotted line) for each of the baseline SnowModel simulations. The observed EC cumulative sublimation is only shown for periods when data were available during the snow-covered period (as determined by snow depth sensors or nearby SNOTEL stations).

sublimation and canopy sublimation rates during that time period determined by this study were 0.32 mm d^{-1} and 0.97 mm d^{-1}, respectively.

Biases between simulated and observed sublimation fluxes could be related to site specific conditions that were not well represented by model simulations or to methodological limitations of EC observations in complex terrain. For example, at the Arrow station, a positive bias in simulated wind speed (supporting infomation Table S5) likely contributed to an overestimation of simulated blowing snow sublimation that was not reported by Sexstone et al. (2016). Conversely, the discrepancy in simulated versus observed sublimation at the T-Van station (station 5503) was more likely related to the representativeness of the *in-situ* EC observations made at 3 m above the surface. In very high wind speeds that are characteristic of the T-Van station, EC sensors located close to the snow surface may neglect blowing snow transport and sublimation that is expected to occur from blowing snow within turbulent suspension (Pomeroy & Male, 1992) up to a height of approximately 10 m above the snow surface (Pomeroy & Gray, 1995). Knowles et al. (2012) assumed that measured EC sublimation from the T-Van station (2007 through 2009) was only representative of surface sublimation, and estimated winter blowing snow sublimation to include an additional 188–281 mm of sublimation, which is similar to the range of simulated blowing snow sublimation at T-Van in this study (78 - 261 mm). Based on this assessment, comparison between EC observations and simulated sublimation excluding blowing snow sublimation can be used to characterize simulated sublimation error.

SnowModel results were compared to streamflow observations and water balance calculations in order to evaluate model performance at the watershed scale. October through July runoff from 11 high-elevation

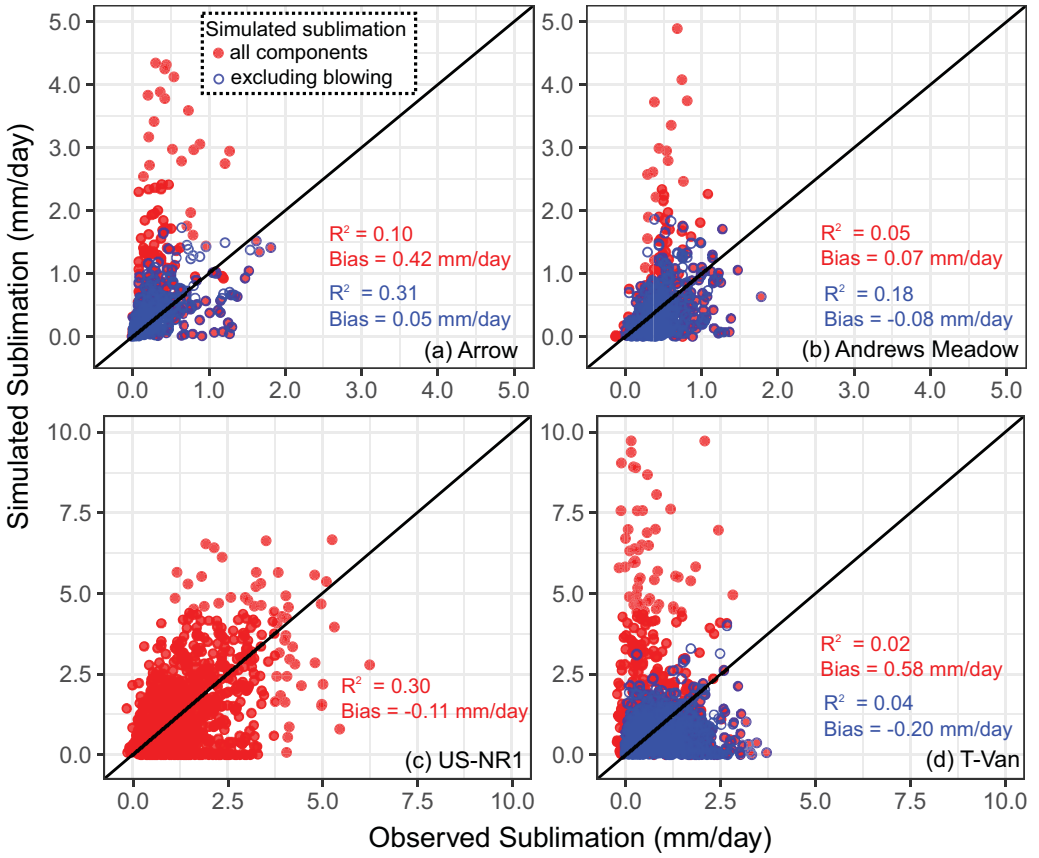

Figure 4. Relation between the observed daily eddy covariance (EC) sublimation flux versus the simulated daily sublimation flux at the (a) Arrow, (b) Andrews Meadow, (c) US-NR1, and (d) T-Van stations. Red filled circles represent all components of simulated sublimation whereas blue open circles exclude the blowing snow sublimation component. The black line represents the 1:1 line.

gaged watersheds that encompassed both alpine and forested areas (Figure 1) averaged 437 mm during the 5-water-year study period (Figure 5). During that time, the average annual simulated watershed precipitation was 946 mm, the mean runoff ratio was 0.45, the mean SSEBop growing season *ET* was 294 mm, and the mean simulated total watershed sublimation was 227 mm. Water balance calculations for each watershed showed significant linear relation ($R^2 = 0.56$; p-value < 0.001) between observed and predicted watershed inputs and outputs (equation (1); Figure 5). Watershed inputs (precipitation) were on average 26 mm less than the watershed outputs (runoff, snow sublimation, blowing snow transport, *ET*); we interpret this residual to represent the combination of changes in watershed storage (not calculated) and uncertainty. However, major changes in watershed storage would not be expected during the October to July period (e.g., Clow et al., 2003). The uncertainty in simulated cumulative precipitation and sublimation ranged from 8 to 17% (supporting infomation Table S6) and from 16 to 35% (mean = 21%) (supporting infomation Table S11), respectively. Based on this error assessment, mean water balance inputs and outputs plus or minus their estimated uncertainty for each year were not significantly different (Taylor, 1997) (Figure 5).

3.2. Sublimation Variability and Importance to the Water Balance

Baseline SnowModel simulations indicated substantial spatial variability of the three components of sublimation across the model domain (Figure 6 and Table 4). Simulated surface sublimation was generally least at the lowest elevations and within forested areas (i.e., sub-canopy), whereas the greatest simulated surface sublimation occurred at the highest elevations in both alpine and forested areas (Figure 6). Coniferous forests dominated the land cover across the domain (section 2.1), and within these high canopy density areas (Figure 1), simulated canopy sublimation increased with increasing elevation, precipitation, and canopy density (i.e., increasing *LAI**) (Figure 6). Canopy sublimation was the dominant simulated sublimation flux in

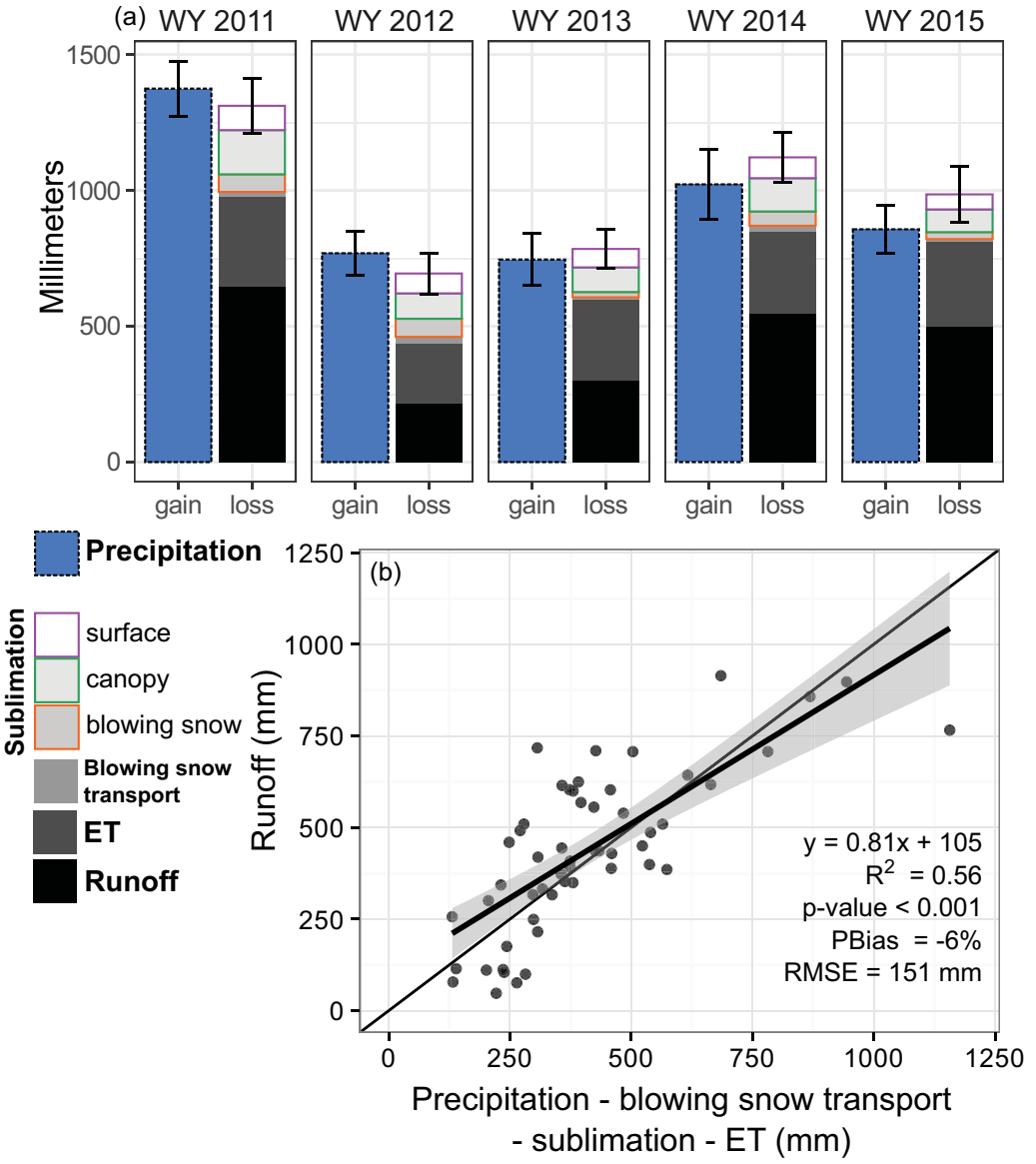

Figure 5. Comparison of water balance components for (a) the average of all watersheds by water year and (b) individual watersheds for each water year; shading represents the 95% confidence level interval of the linear regression. Water balance components represent October–July of each water year. The error bars in (a) correspond to measurement uncertainty.

the baseline simulations, accounting for 58% of total sublimation losses to the atmosphere on average across the model domain. Simulated blowing snow sublimation was limited to non-forested areas and generally increased with elevation and was greatest in alpine areas (Figure 6). Simulated blowing snow sublimation losses were moderate when averaged across the model domain (Table 4); however, localized totals on exposed alpine ridges reached up to 450 mm when averaged across all years (Figure 6). Across the model domain, the mean simulated total sublimation (sum of surface, canopy, and blowing snow sublimation) was greatest at the highest elevations with substantial sublimation losses in both subalpine and alpine areas (Figure 6).

Total simulated winter (1 October through 31 May) precipitation was variable from year-to-year, and decreased by a factor of 1.8 from the wettest year (WY 2011) to the driest year (WY 2012) of the study (Table 4). Total simulated sublimation was generally greatest in years with the greatest simulated winter precipitation and snow cover duration and also linearly related with simulated mean vapor pressure gradient

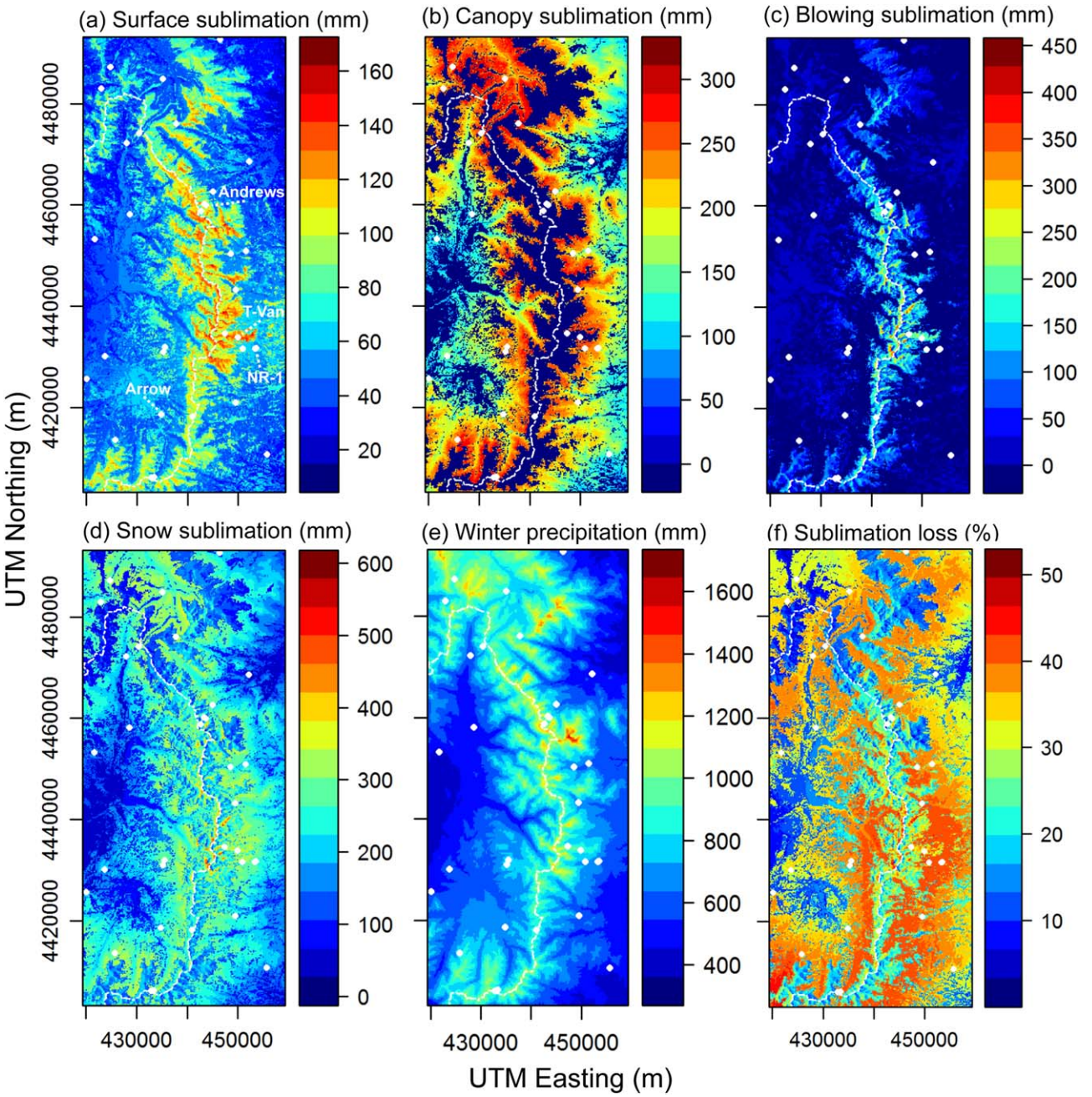

Figure 6. Spatial variability of the 5 year simulated mean (a) total surface sublimation, (b) total canopy sublimation, (c) total blowing snow sublimation, (d) total snow sublimation, (e) total winter precipitation, and (f) the percent of winter precipitation that was sublimated across the model domain. White circles show meteorological evaluation stations and the dashed white line shows the Continental Divide. Note the scale change with each panel.

between the snow and the atmosphere ($R^2 = 0.71$; p-value < 0.1) and the simulated mean wind speed ($R^2 = 0.77$; p-value < 0.1) (Table 4). On average, 28% of simulated winter precipitation was sublimated. This percentage was generally greatest in years with lower winter precipitation and/or snow cover duration (Table 4). The sublimation/precipitation ratio (relative sublimation loss; Figure 6f) was strongly linked to the distribution of land cover type. Although mean annual simulated sublimation was substantial in alpine areas (Figure 7), this flux accounted for a relatively greater percentage of winter precipitation within forested areas due to significant canopy sublimation (Figure 7). The mean simulated sublimation within open areas below treeline included a moderate contribution from surface sublimation as well as a small contribution from blowing snow sublimation and was 33% and 133% less than the mean simulated sublimation from

Table 4
Total and Component Simulated Sublimation, Simulated Days With Greater Than 20% Domain Snow Cover, Total Winter (1 October to 31 May) Simulated Precipitation, Percentage of Simulated Winter Precipitation Lost to the Atmosphere by Simulated Sublimation, Mean Winter Vapor Pressure Gradient Between the Snowpack and the Atmosphere, Mean Winter Available Energy for Turbulent Flux, and Mean Winter Wind Speed Across the Model Domain for Each Water Year of the Modeling Study

Water year	2011	2012	2013	2014	2015	Mean	Std dev
Surface sublimation (mm)	74	59	54	68	45	60	11
Canopy sublimation (mm)	153	95	97	130	91	113	27
Blowing snow sublimation (mm)	34	34	10	28	13	24	12
Total sublimation (mm)	260	187	161	225	149	196	46
Snow cover > 20% (days)	266	219	230	258	236	242	20
Winter precipitation (mm)	932	515	592	806	681	705	167
Sublimation loss (%)	28	36	27	28	22	28	5
Vapor pressure gradient (Pa)	15.1	9.4	9.9	14.8	0.2	9.9	6.1
Available energy (W m^{-2})	12.3	13.3	11.9	10.6	11.0	11.8	1.1
Wind speed (m s^{-1})	3.9	3.7	3.5	3.8	3.1	3.6	0.3

alpine and forested areas, respectively (Figure 7). Considering the land cover distribution of the model domain (approximately 22% alpine, 58% forest, and 20% open below treeline), it is evident that sublimation fluxes from forested areas are particularly important to the integrated snow mass balance across the model domain. Accordingly, this work highlights the value of future experimental designs that represent sublimation from both alpine and forested areas, as well as forest openings below treeline.

A key finding of this research is that 28% of winter precipitation was sublimated to the atmosphere over a 5 year period in the north-central Colorado Rocky Mountains. For comparison, another recent modeling study that simulated the spatio-temporal variability of sublimation showed that spatial variations of sublimation ranged from 10 to 90% of annual snowfall, but averaged 22% across Berchtesgaden National Park, Germany (Strasser et al., 2008). Both the current study and Strasser et al. (2008) highlight that domain-averaged canopy sublimation represents the greatest sublimation loss, followed by surface sublimation, then blowing snow sublimation (Table 4). For context, MacDonald et al. (2010) estimated sublimation losses to account for 20 to 32% of cumulative snowfall in an alpine region of the Canadian Rocky Mountains, and Gascoin et al. (2013) suggested that sublimation accounted for 71% of total snowpack ablation in the Dry Andes of Chile. Higher sublimation fluxes shown by Gascoin et al. (2013) were the combined result of low precipitation, an arid climate, high wind speed, and exposed topography. The results presented herein contribute to refining our understanding of the watershed-scale importance of sublimation in semi-arid mountain regions around the world, and highlight the importance of both total winter precipitation as well as meteorological forcing conditions to the interannual variability of both total and relative fluxes (Table 4).

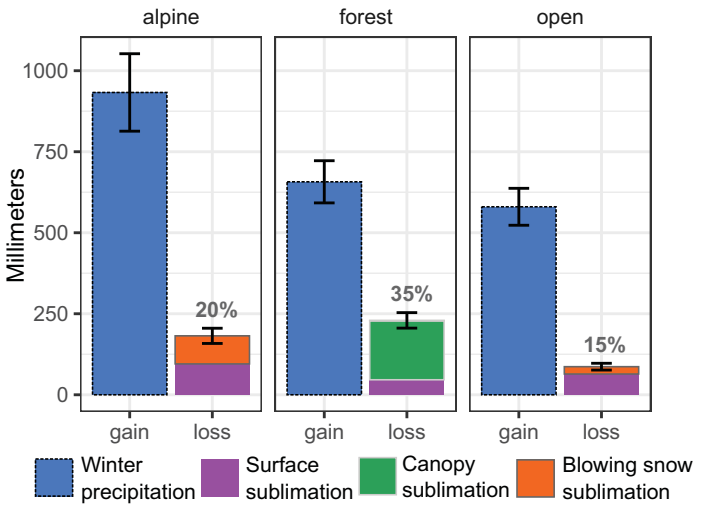

Figure 7. Comparison of the 5 year simulated mean sublimation flux to simulated winter precipitation within the alpine, forest, and open land cover types. The percentage listed above the "loss" column represents the percentage of winter precipitation that was sublimated within each land cover type. Error bars denote the 5 year standard error of the mean.

3.3. Sensitivity to Bark-Beetle Forest Disturbance

Bark-beetle disturbance simulations indicated an overall minor decrease in simulated sublimation from forested areas when compared to the baseline simulations (Figure 8a). Specifically, simulated sublimation losses from forested areas across the model domain were reduced by 8 mm (or 4%) in response to the *LAI** reduction that was prescribed to represent current bark-beetle conditions. The simulated sublimation reduction was a product of decreased canopy sublimation (−12 mm; −7%) but increased surface sublimation (4 mm; 9%) (Figure 8a). The mean domain-wide difference in simulated daily sublimation rates between the baseline and bark-beetle simulations was −0.03 mm d^{-1} (Wilcoxon signed-rank test p-value < 0.001).

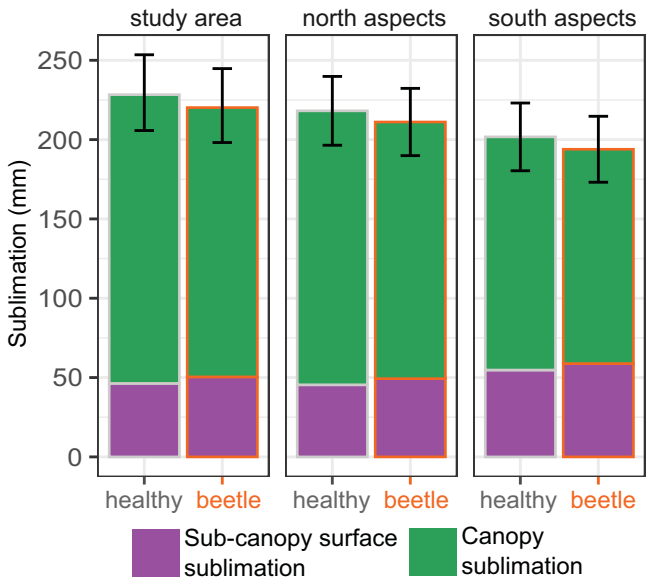

Figure 8. Comparison of the 5 year mean simulated total sublimation and individual sublimation components from forested areas modeled by the baseline and bark-beetle (*LAI** reduction) SnowModel simulations. The error bars on each column represent the 5 year standard error of the mean.

Decreased simulated canopy sublimation in the presence of bark-beetle disturbance resulted from a reduction in canopy intercepted snow that was consistent throughout the snow season (Figure 9). In contrast, increased simulated surface sublimation in the bark-beetle scenario was a more complex response caused by changes to the sub-canopy radiation balance and available energy, increased sub-canopy wind speeds, and a decreased vapor pressure gradient between the sub-canopy snow and the atmosphere. The *LAI** reduction in the bark-beetle scenario yielded increased simulated incoming shortwave radiation that increased throughout the snow season (Figure 9). However, simulated incoming and outgoing longwave radiation (i.e., snow surface temperature) consistently decreased throughout the snow season, which outweighed the incoming shortwave radiation increases, and yielded a decrease in net radiation during the majority of the winter period (Figure 9). The overall simulated available energy for turbulent flux was consistently higher in the bark-beetle scenario, and the mean simulated sub-canopy wind speeds were 5% greater (Figure 9). However, the simulated vapor pressure gradient between the snow surface and the atmosphere decreased in the bark-beetle scenario in proportion to simulated snow surface temperatures that consistently decreased as a result of snow energy balance changes that yielded a lower vapor pressure at the snow surface (Figure 9). Therefore, increased simulated sub-canopy sublimation was promoted by greater available energy for turbulent flux and greater sub-canopy wind speeds, but also damped by the decreased snow-atmosphere vapor pressure gradient.

Given the potential importance of the radiation balance to forest sublimation in the presence of disturbance (e.g., Biederman et al., 2014; Harpold et al., 2014), we assessed the variability of simulated forest sublimation

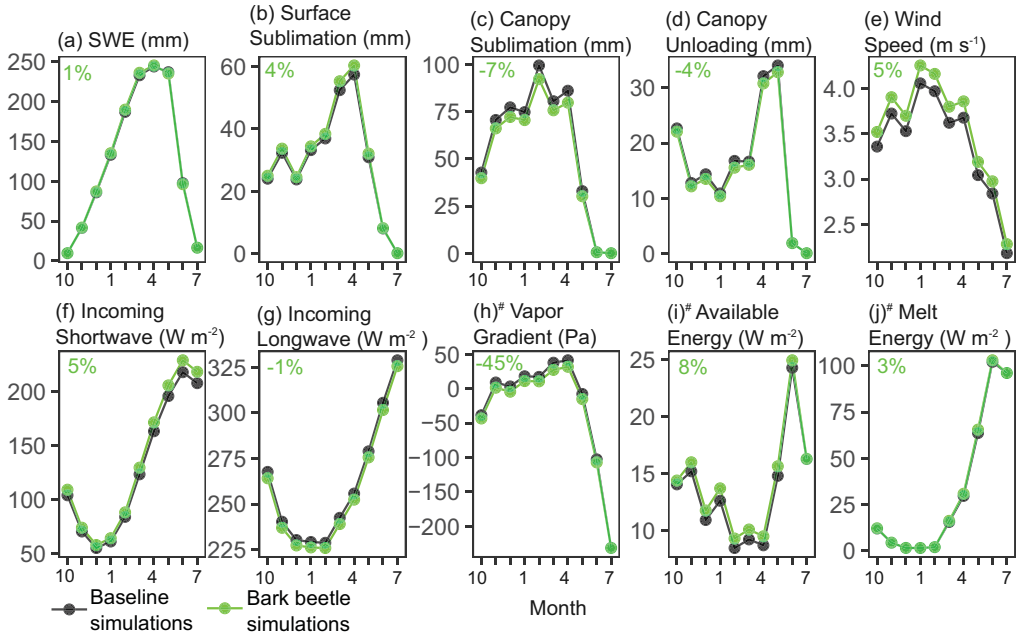

Figure 9. Comparison of monthly simulated (a) mean SWE, (b) total surface sublimation, (c) total canopy sublimation, (d) total canopy unloading, (e) mean wind speed, (f) incoming shortwave radiation, (g) incoming longwave radiation, (h) mean vapor pressure gradient between the snow and the atmosphere, (i) mean available energy for turbulent flux, and (j) mean energy available for melt for the baseline and bark-beetle simulations. The percentages listed in each panel represent the percent difference between the yearly averages of each variable from the baseline scenario. #Denotes that the percent difference calculations are based on November–May as opposed to the yearly average.

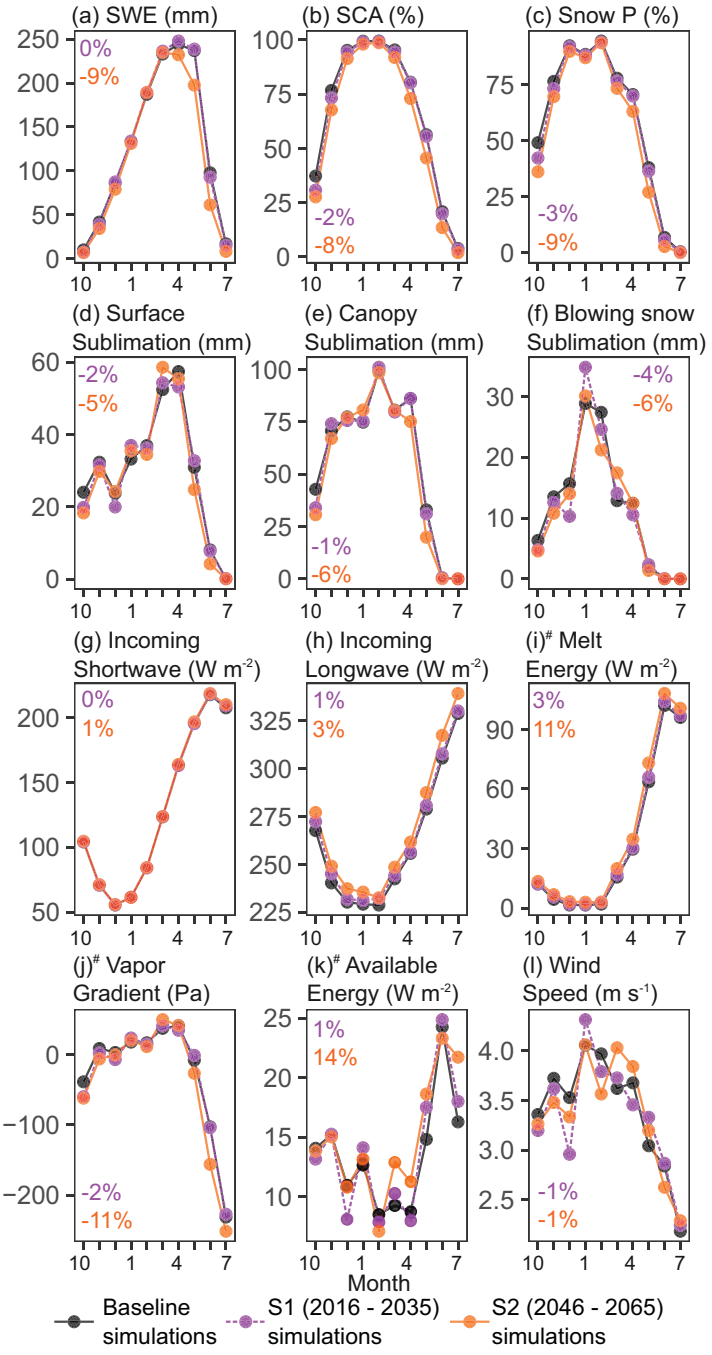

Figure 10. Comparison of monthly simulated (a) mean snow water equivalent (SWE), (b) snow covered area (SCA), (c) mean percentage of precipitation falling as snow, (d) total surface sublimation, (e) total canopy sublimation, (f) total blowing snow sublimation, (g) mean incoming shortwave radiation, (h) mean incoming longwave radiation, (i) mean energy available for melt, (j) mean vapor pressure gradient between the snow and the atmosphere, (k) mean available energy for turbulent flux, and (l) mean wind speed for the baseline and S1 and S2 climate change simulations. The percentages listed in each panel represent the percent difference between the yearly averages of each variable from the baseline scenario. #Denotes that the percent difference calculations are based on November–May.

between south facing (135°–225°) and north facing (315°–45°) aspects (Figures 8b and 8c). Comparing south- to north-facing aspects, surface sublimation was 16% greater, canopy sublimation was 20% less, and total sublimation was 9% less in the bark-beetle scenario. However, the south- and north-facing surface and canopy sublimation responses to bark-beetle disturbance were not significantly different from the domain-wide average, consistently demonstrating a minor decrease in simulated sublimation (Figures 8b and 8c).

In the context of previous research, these results allow for new insight specific to the mechanisms that may be important for driving sublimation processes in the presence of disturbance. In particular, the modeled reduction in simulated canopy sublimation was comparable to a recent modeling study from a low-latitude mountainous watershed in Arizona (Svoma, 2017). Additionally, the simulated increase in sub-canopy surface sublimation was similar in magnitude to an estimation in the Colorado Rocky Mountains (Penn et al., 2016), but opposite in sign to that of Svoma (2017). Given that the decrease in sub-canopy surface sublimation simulated by Svoma (2017) was attributed to decreased incoming longwave radiation from the forest canopy, the sub-canopy surface sublimation response to bark-beetle disturbance may vary from low to mid-latitudes. Taken together, recent studies have highlighted that sub-canopy surface sublimation increases can be equal to or greater than canopy sublimation decreases in catchments subject to beetle- or fire-induced tree mortality (Biederman et al., 2014; Harpold et al., 2014); this result was not produced in the current study and suggests that site-specific changes to the sublimation forcing mechanisms are likely important to the overall sublimation response. The overall 4% decrease in simulated sublimation due to bark-beetles identified by this work is generally a smaller decrease than results from other modeling experiments in the Rocky Mountains that showed an overall decrease in annual ET (e.g., Chen et al., 2015; Livneh et al., 2015; Penn et al., 2016). Since the simulated water balance in this study (Figure 5) suggested that sublimation fluxes and growing season ET were equivalent to 52% and 67% of runoff, an overall 4% decrease in simulated sublimation would account for an increase in water available for snowmelt equivalent to 2% of watershed runoff. Given that Livneh et al. (2015) show an annual decrease in simulated ET (including sublimation) of approximately 15% in a comparable bark-beetle scenario, and that Chen et al. (2015) and Penn et al. (2016) highlight a 10–11% reduction in ET, our results imply that decreases in growing season ET are likely to be greater in magnitude than decreases in sublimation. Accordingly, the results of this study contribute to a more refined understanding of how changing sublimation dynamics may affect the integrated hydrologic response of bark-beetle disturbance-affected watersheds (e.g., Bearup et al., 2014; Biederman et al., 2015).

3.4. Sensitivity to Climate Warming

SnowModel simulations representing future climate conditions indicated an overall 2% decrease in simulated sublimation in the S1 scenario (2016–2035) and a 6% decrease in the S2 scenario (2046–2065). Each component of simulated sublimation decreased in the future warming conditions. Simulated surface sublimation decreased by 2% and 5%, canopy sublimation decreased by 1% and 6%, and blowing

snow sublimation decreased by 4% and 6% in the S1 and S2 scenarios, respectively (Figure 10). The mean domain-wide differences in simulated daily sublimation rates between the baseline and S1 and S2 simulations were -0.01 mm d^{-1} and -0.02 mm d^{-1} (Wilcoxon signed-rank test p-value < 0.001).

The simulated mean peak SWE increased by 2% in the S1 scenario but decreased by 5% in the S2 scenario. In contrast, snow cover duration decreased in both scenarios as a result of both greater energy available for melt and a decrease in the fraction of snow precipitation (Figure 10). The available energy for turbulent flux increased by 1% in the S1 scenario and by 14% in the S2 scenario; however, the simulated vapor pressure gradient between the snow and the atmosphere decreased by 2% in the S1 scenario and by 11% in the S2 scenario, as a result of greater atmospheric vapor pressure due to warming climate conditions (Figure 10). Additionally, simulated wind speeds were on average 1% less than baseline conditions in the S1 and S2 scenarios. Therefore, despite greater available energy for turbulent flux in the warming climate scenarios, the overall decrease in simulated sublimation totals in the S1 and S2 scenarios resulted from a reduction in simulated snow cover duration, vapor pressure gradients, and wind speed.

In order to remove the influence of snow cover duration, we also restricted the sublimation response to changing climate analysis to time periods with snow-covered conditions. Therefore, the simulated daily mean sublimation rate was computed for snow-covered areas only during the mid-winter months of January–April for each of the baseline and future climate scenarios. The distribution of simulated sublimation rates for each scenario was further subset into four elevation zones, to assess the elevational sensitivity of mid-winter sublimation rates in the future (Figure 11). Across the domain, the simulated sublimation rates did not change from the baseline to S1 scenarios, and were increased by 1% between the baseline to S2 scenarios. While the lowest elevations showed minor increases (1%) in simulated sublimation for both climate scenarios, simulated sublimation at the middle elevations slightly decreased (1%) in the S1 scenario but modestly increased (2%) in the S2 scenario (Figure 11). At the highest elevations (alpine), simulated sublimation rates decreased for both the S1 (<1%) and S2 (1%) scenarios (Figure 11). For each of the elevation zones, the largest magnitude change in simulated sublimation was an increase at the highest sublimation rates (95th percentile) (Figure 11).

Results from the climate warming sensitivity simulations highlight that sublimation rates are expected to be similar or slightly increased in the future. However, given that snow cover duration is projected to decrease, total sublimation fluxes are also expected to decrease by up to 6%. Therefore, the net result of earlier, slower snowmelt (e.g., Clow, 2010; Musselman et al., 2017), and potential future shifts in the percentage of snow versus rain (e.g., Trujillo & Molotch, 2014), may lead to similar or slightly increased future sublimation fluxes in this region. These results differ from a recent study that highlighted the potential for significant decreases to sublimation fluxes due to changing climate conditions in the Reynolds Creek Experimental Watershed, Idaho (Rasouli et al., 2015). As a possible explanation for this difference, we invoke the relative humidity perturbation prescribed in our climate change experiments (Table 2). Climate model projections often assume constant relative humidity with increasing air temperature because higher surface temperatures increase evaporation over oceans (Dessler & Sherwood, 2009). However, over arid and semi-arid landscapes that are subject to seasonal moisture limitation, future relative humidity decreases are expected (Pierce et al., 2013), and were included in the dynamically downscaled RegCM3 GCM simulations prescribed by this study (Table 2). These relative humidity decreases were important for damping the simulated decreases in vapor pressure gradient between the snow and the atmosphere (Figure 10). Given that recent work has highlighted the importance of sublimation fluxes to snowpack resiliency in arid and semi-arid environments (Harpold & Brooks, 2018; López-Moreno et al., 2017), this study evaluated the role of sublimation, in order to contextualize the integrated snowpack response to changing climate conditions.

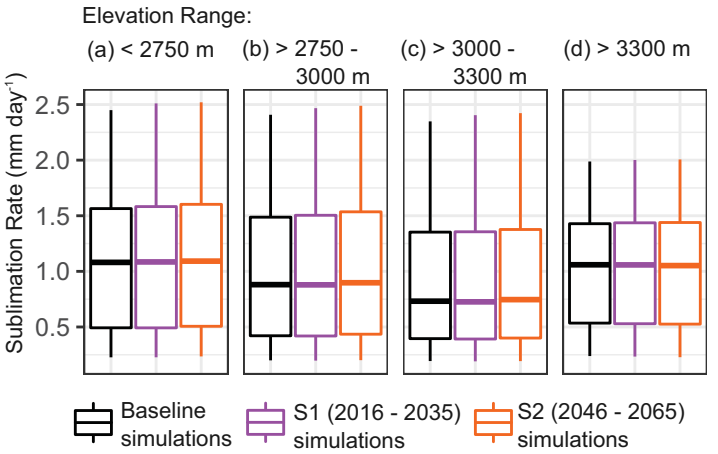

Figure 11. Boxplots of mean daily simulated sublimation rates from the baseline, S1, and S2 simulations for areas covered by snow during January through July and elevations ranging (a) < 2,750 m, (b) > 2,750–3,000 m, (c) > 3,000–3,300 m, (d) > 3300 m. Boxplots are represented by the 5th and 95th percentiles (whiskers), 25th and 75th percentiles (box) and median (horizontal line).

3.5. Sublimation Modeling Uncertainty

The evaluation of simulated sublimation using EC observations presented by this work indicates that SnowModel is able to realistically

represent the seasonal evolution and magnitude of surface and canopy sublimation within or near the range of EC measurement uncertainty (Knowles et al., 2012, 2015; Sexstone et al., 2016; Figure 3). An error analysis of simulated sublimation (excluding simulated blowing snow sublimation) suggests that uncertainty in simulated sublimation ranged from 16 to 35% (mean = 21%). These biases are comparable to previous modeling studies in the region (e.g., Broxton et al., 2015; Mahat et al., 2013; Svoma, 2017). However, this model evaluation also highlighted potential limitations in modeling specific site conditions, particularly in complex terrain and alpine environments where substantial blowing snow occurs. Given that model verification of blowing snow sublimation was not possible with the experimental design of this study, blowing snow sublimation is an important source of uncertainty in simulated sublimation estimates. These findings suggest that future investigations capable of measuring both surface and blowing snow sublimation fluxes in alpine regions are needed to better constrain total sublimation estimates in the mountains.

Uncertainty associated with the sublimation model (supporting information Text S1) could also have affected the results of this work. Recent advances in LiDAR data collection capabilities have led to advances in model representations of canopy snow interactions (Broxton et al., 2015; Moeser et al., 2015; Musselman et al., 2013). The current study represents canopy conditions across 100 m grid cells based on an estimated *LAI**, which may produce uncertainty resultant from unresolved sub-grid canopy structure and associated canopy interception and sublimation (Moeser et al., 2016). Additionally, SnowModel unloads melting snow from the canopy (Liston & Elder, 2006b), and this study implemented a continuous unloading scheme (Mahat & Tarboton, 2014) during cold conditions to represent unloading of snow by wind and bending of branches (supporting information Text S1). However, field observations of canopy unloading within the study area suggest that these events are episodic and can unload substantial amounts of snow in short amounts of time; therefore, they are not likely to be well represented within the model.

Uncertainty associated with modeling the spatial variability of sublimation can be directly related to uncertainty in the spatially interpolated meteorological forcing data, particularly wind speed and relative humidity (Dadic et al., 2013; Raleigh et al., 2015). This study completed a rigorous error assessment of simulated meteorological forcing variables using station observations, and highlighted biases in relative humidity and wind speed that likely contributed to the simulated sublimation uncertainty. Gascoin et al. (2013) found that the windflow model used by SnowModel (Liston et al., 2007) accurately represented synoptic wind conditions in high elevation areas, but that the model was not able to represent windflow important in valley locations that are increasingly influenced by local topography and diurnal variability. Musselman et al. (2015) evaluated three windflow models, including that of Liston et al. (2007), and found that the snow mass balance was highly sensitive to the model configuration; differences in simulated windflow produced a range of blowing snow sublimation from 10.5% to 19% of seasonal snowfall (Musselman et al., 2015). As a result, we recommend that future studies seeking to simulate sublimation fluxes rigorously evaluate and consider bias correcting meteorological forcing data to minimize model uncertainty.

4. Conclusions

Model evaluation based on snow and micrometeorological observations, water balance calculations, and comparisons to previous work were used to show that SnowModel reasonably represented the seasonal evolution and magnitude of sublimation within a 3,600 km^2 model domain in the Colorado Rocky Mountains. The resulting simulated sublimation flux was equivalent to an average of 28% of winter precipitation. Although the magnitude of annual sublimation increased with increasing winter precipitation, the importance of sublimation (as a percentage of winter precipitation) increased in low snow years. The spatial variability of sublimation was controlled by the interaction of meteorology (e.g., available energy, vapor pressure gradient, and wind speed), topographic position, and variations in land cover type and physiography. The highest simulated sublimation rates occurred in alpine (20% of winter precipitation) and forested areas (35% of winter precipitation), and relatively lower rates occurred in open areas below treeline (15% of winter precipitation). Across the model domain, sublimation from forested areas dominated water vapor losses from the snowpack, indicating the importance of canopy sublimation in this region. Model simulations that incorporated an *LAI** reduction due to bark-beetle-induced forest mortality within the study area showed a 4% decrease in the sublimation flux from forested areas, which was the product of decreased canopy sublimation but increased sub-canopy surface sublimation. Although model simulations representing

future climate conditions highlighted that future sublimation rates in this region are likely to remain unchanged or to slightly increase, total sublimation losses are expected to decrease by up to 6% due to a reduction in snow covered area and duration. This work therefore suggests that uncertainty in modeled sublimation may be particularly sensitive to the ability of a given snow model to accurately simulate precipitation phase and amount and, thus, domain-wide snow cover duration, which was well validated in this study. These results constrain the importance of surface, canopy, and blowing snow sublimation components to the water balance of a semi-arid, mountainous region during winter, and can be used to inform future decision making and water management practices.

Acknowledgments

All data including modeled outputs have been archived in a USGS ScienceBase data release and are publically accessible at https://doi.org/10.5066/F75M64QQ. This study was supported by the USGS Water Availability and Use Science Program and the USGS Climate and Land Use Change Program. John Knowles was additionally supported by NSF grant DEB 1027341 to the Niwot Ridge LTER. We would like to acknowledge the AmeriFlux program, the Natural Resource Conservation Service, DRI Western Regional Climate Center, the Niwot Ridge LTER Program, and the Colorado Avalanche Information Center for providing the high-quality data used in this study. Thanks to Sean Burns (University of Colorado Boulder) for help with the US-NR1 data sets. We would also like to thank David Moeser (USGS) and four anonymous reviewers for their insightful comments that improved this manuscript. Any use of trade, firm, or product names is for descriptive purposes only and does not imply endorsement by the U.S. Government.

References

Andreas, E. L., Persson, P. O. G., Jordan, R. E., Horst, T. W., Guest, P. S., Grachev, A. A., & Fairall, C. W. (2010). Parameterizing turbulent exchange over sea ice in winter. *Journal of Hydrometeorology*, *11*, 87–104. https://doi.org/10.1175/2009jhm1102.1

Bales, R. C., Molotch, N. P., Painter, T. H., Dettinger, M. D., Rice, R., & Dozier, J. (2006). Mountain hydrology of the western United States. *Water Resources Research*, *42*, W08432. https://doi.org/10.1029/2005WR004387

Bearup, L. A., Maxwell, R. M., Clow, D., & McCray, J. E. (2014). Hydrological effects of forest transpiration loss in bark beetle-impacted watersheds. *Nature Climate Change*, *4*, 481–486. https://doi.org/10.1038/nclimate2198

Biederman, J. A., Brooks, P. D., Harpold, A. A., Gochis, D. J., Gutmann, E., Reed, D. E., et al. (2014). Multiscale observations of snow accumulation and peak snowpack following widespread, insect-induced lodgepole pine mortality. *Ecohydrology*, *7*, 150–162. https://doi.org/10.1038/nclimate219810.1002/eco.1342.

Biederman, J. A., Somor, A. J., Harpold, A. A., Gutmann, E. D., Breshears, D. D., Troch, P. A., et al. (2015). Recent tree die-off has little effect on streamflow in contrast to expected increases from historical studies. *Water Resources Research*, *51*, 9775–9789. https://doi.org/10.1002/2015WR017401

Boon, S. (2012). Snow accumulation following forest disturbance. *Ecohydrology*, *5*, 279–285. https://doi.org/10.1002/eco.212

Bright, B. C., Hicke, J. A., & Meddens, A. J. H. (2013). Effects of bark beetle-caused tree mortality on biogeochemical and biogeophysical MODIS products. *Journal ofGeophysical Research: Biogeosciences*, *118*, 974–982. https://doi.org/10.1002/jgrg.20078

Broxton, P. D., Harpold, A. A., Biederman, J. A., Troch, P. A., Molotch, N. P., & Brooks, P. D. (2015). Quantifying the effects of vegetation structure on snow accumulation and ablation in mixed-conifer forests. *Ecohydrology*, *8*, 1073–1094. https://doi.org/10.1002/eco.1565

Burns, S. P., Molotch, N. P., Williams, M. W., Knowles, J. F., Seok, B., Monson, R. K., et al. (2014). Snow temperature changes within a seasonal snowpack and their relationship to turbulent fluxes of sensible and latent heat. *Journal of Hydrometeorology*, *15*, 117–142. https://doi.org/10.1175/JHM-D-13-026.1

Chen, F., Zhang, G., Barlage, M., Zhang, Y., Hicke, J. A., Meddens, A., et al. (2015). An observational and modeling study of impacts of bark beetle-caused tree mortality on surface energy and hydrological cycles. *Journal of Hydrometeorology*, *16*, 744–761. https://doi.org/10.1175/JHM-D-14-0059.1

Cline, D. W. (1997). Snow surface energy exchanges and snowmelt at a continental, midlatitude Alpine site. *Water Resources Research*, *33*, 689–701. https://doi.org/10.1029/97WR00026

Clow, D. W. (2010). Changes in the timing of snowmelt and streamflow in Colorado: A response to recent warming. *Journal of Climate*, *23*, 2293–2306. https://doi.org/10.1175/2009JCLI2951.1

Clow, D. W., Schrott, L., Webb, R., Campbell, D. H., Torizzo, A., & Dornblaser, M. (2003). Ground water occurrence and contributions to streamflow in an alpine catchment, Colorado Front Range. *Ground Water*, *41*, 937–950. https://doi.org/10.1111/j.1745-6584.2003.tb02436.x

Dadic, R., Mott, R., Lehning, M., Carenzo, M., Anderson, B., & Mackintosh, A. (2013). Sensitivity of turbulent fluxes to wind speed over snow surfaces in different climatic settings. *Advances in Water Resources*, *55*, 178–189. https://doi.org/10.1016/j.advwatres.2012.06.010

Dery, S. J., Taylor, P. A., & Xiao, J. B. (1998). The thermodynamic effects of sublimating, blowing snow in the atmospheric boundary layer. *Boundary Layer Meteorology*, *89*, 251–283. https://doi.org/10.1023/A:1001712111718

Dessler, A. E., & Sherwood, S. C. (2009). A matter of humidity. *Science*, *323*, 1020–1021. https://doi.org/10.1126/science.1171264

Elder, K., Dozier, J., & Michaelsen, J. (1991). Snow accumulation and distribution in an alpine watershed. *Water Resources Research*, *27*, 1541–1552. https://doi.org/10.1029/91WR00506

Fassnacht, S. R. (2004). Estimating alter-shielded gauge snowfall undercatch, snowpack sublimation, and blowing snow transport at six sites in the coterminous USA. *Hydrological Processes*, *18*, 3481–3492. https://doi.org/10.1002/hyp.5806

Gascoin, S., Lhermitte, S., Kinnard, C., Bortels, K., & Liston, G. E. (2013). Wind effects on snow cover in Pascua-Lama, Dry Andes of Chile. *Advances in Water Resources*, *55*, 25–39. https://doi.org/10.1016/j.advwatres.2012.11.013

Goodison, B., Louie, P., & Yang, D. (1998). WMO solid precipitation measurement intercomparison final report (WMO Instruments and Observing Methods Rep. 67, WMO/TD 872). Geneva, Switzerland: World Meteorological Organization.

Greene, E. M., Liston, G. E., & Pielke, R. A. (1999). Simulation of above treeline snowdrift formation using a numerical snow-transport model. *Cold Regions Science and Technology*, *30*, 135–144. https://doi.org/10.1016/S0165-232X(99)00008-7

Groot Zwaaftink, C. D., Mott, R., & Lehning, M. (2013). Seasonal simulation of drifting snow sublimation in Alpine terrain. *Water Resources Research*, *49*, 1581–1590. https://doi.org/10.1002/wrcr.20137

Gustafson, J. R., Brooks, P. D., Molotch, N. P., & Veatch, W. C. (2010). Estimating snow sublimation using natural chemical and isotopic tracers across a gradient of solar radiation. *Water Resources Research*, *46*, W12511. https://doi.org/10.1029/2009WR009060

Harpold, A., Brooks, P., Rajagopal, S., Heidbuchel, I., Jardine, A., & Stielstra, C. (2012). Changes in snowpack accumulation and ablation in the intermountain west. *Water Resources Research*, *48*, W11501. https://doi.org/10.1029/2012WR011949

Harpold, A. A., Biederman, J. A., Condon, K., Merino, M., Korgaonkar, Y., Nan, T. C., et al. (2014). Changes in snow accumulation and ablation following the Las Conchas Forest Fire, New Mexico, USA. *Ecohydrology*, *7*, 440–452. https://doi.org/10.1002/eco.1363

Harpold, A. A., & Brooks, P. D. (2018). Humidity determines snowpack ablation under a warming climate. *Proceedings of the National Academy of Sciences of the United States of America.*, *115*(6), 1215–1220. https://doi.org/10.1073/pnas.1716789115

Hedstrom, N. R., & Pomeroy, J. W. (1998). Measurements and modelling of snow interception in the boreal forest. *Hydrological Processes*, *12*, 1611–1625. https://doi.org/10.1002/(SICI)1099-1085(199808/09)12:10/11<1611::AID-HYP684>3.0.CO;2-4

Helgason, W., & Pomeroy, J. (2012). Problems closing the energy balance over a homogeneous snow cover during midwinter. *Journal of Hydrometeorology*, *13*, 557–572. https://doi.org/10.1175/JHM-D-11-0135.1

Hiemstra, C. A., Liston, G. E., & Reiners, W. A. (2006). Observing, modelling, and validating snow redistribution by wind in a Wyoming upper treeline landscape. *Ecological Modelling*, *197*, 35–51. https://doi.org/10.1016/j.ecolmodel.2006.03.005

Homer, C., Dewitz, J., Yang, L. M., Jin, S., Danielson, P., Xian, G., et al. (2015). Completion of the 2011 national land cover database for the conterminous United States-–Representing a decade of land cover change information. *Photogrammetric Engineering & Remote Sensing*, *81*, 345–354. https://doi.org/10.14358/Pers.81.5.345

Hood, E., Williams, M., & Cline, D. (1999). Sublimation from a seasonal snowpack at a continental, mid-latitude alpine site. *Hydrological Processes*, *13*, 1781–1797. https://doi.org/10.1002/(SICI)1099-1085(199909)13:12/13<1781::AID-HYP860>3.0.CO;2-C

Hostetler, S. W., Alder, J. R., & Allan, A. M. (2011). Dynamically downscaled climate simulations over North America: Methods, evaluation, and supporting documentation for users. *U.S. Geological Survey Open-File Report, 2011-1238*, 64 pp.

Kashipazha, A. H. (2012). *Practical snow depth sampling around six snow telemetry (SNOTEL) stations in Colorado and Wyoming, United States* (M.S. thesis, 189 pp.). Fort Collins, CO: Colorado State University.

Kattelmann, R., & Elder, K. (1991). Hydrologic characteristics and water-balance of an alpine basin in the Sierra-Nevada. *Water Resources Research*, *27*, 1553–1562. https://doi.org/10.1029/90WR02771

Knowles, J. F., Blanken, P. D., Williams, M. W., & Chowanski, K. M. (2012). Energy and surface moisture seasonally limit evaporation and sublimation from snow-free alpine tundra. *Agricultural and Forest. Meteorology*, *157*, 106–115. https://doi.org/10.1016/j.agrformet.2012.01.017

Knowles, J. F., Harpold, A. A., Cowie, R., Zeliff, M., Barnard, H. R., Burns, S. P., et al. (2015). The relative contributions of alpine and subalpine ecosystems to the water balance of a mountainous, headwater catchment. *Hydrological Processes*, *29*, 4794–4808. https://doi.org/10.1002/hyp.10526

Knowles, N., Dettinger, M. D., & Cayan, D. R. (2006). Trends in snowfall versus rainfall in the Western United States. *Journal of Climate*, *19*, 4545–4559. https://doi.org/10.1175/JCLI3850.1

Lehning, M., Volksch, I., Gustafsson, D., Nguyen, T. A., Stahli, M., & Zappa, M. (2006). ALPINE3D: A detailed model of mountain surface processes and its application to snow hydrology. *Hydrological Processes*, *20*, 2111–2128. https://doi.org/10.1002/hyp.6204

Liston, G. E. (1995). Local advection of momentum, heat, and moisture during the melt of patchy snow covers. *Journal of Applied Meteorology*, *34*, 1705–1715. https://doi.org/10.1175/1520-0450-34.7.1705

Liston, G. E., & Elder, K. (2006a). A meteorological distribution system for high-resolution terrestrial modeling (MicroMet). *Journal of Hydrometeorology*, *7*, 217–234. https://doi.org/10.1175/JHM486.1

Liston, G. E., & Elder, K. (2006b). A distributed snow-evolution modeling system (SnowModel). *Journal of Hydrometeorology*, *7*, 1259–1276. https://doi.org/10.1175/JHM548.1

Liston, G. E., Haehnel, R. B., Sturm, M., Hiemstra, C. A., Berezovskaya, S., & Tabler, R. D. (2007). Instruments and methods simulating complex snow distributions in windy environments using SnowTran-3D. *Journal of Glaciology*, *53*, 241–256. https://doi.org/10.3189/172756507782202865

Liston, G. E., & Hall, D. K. (1995). An energy-balance model of lake-ice evolution. *Journal of Glaciology*, *41*, 373–382.

Liston, G. E., & Hiemstra, C. A. (2011). The changing cryosphere: Pan-arctic snow trends (1979–2009). *Journal of Climate*, *24*, 5691–5712. https://doi.org/10.1175/JCLI-D-11-00081.1

Liston, G. E., Hiemstra, C. A., Elder, K., & Cline, D. W. (2008). Mesocell study area snow distributions for the Cold Land Processes Experiment (CLPX). *Journal of Hydrometeorology*, *9*, 957–976. https://doi.org/10.1175/2008JHM869.1

Liston, G. E., & Sturm, M. (1998). A snow-transport model for complex terrain. *Journal of Glaciology*, *44*, 498–516.

Liston, G. E., & Sturm, M. (2004). The role of winter sublimation in the Arctic moisture budget. *Nordic Hydrology*, *35*, 325–334.

Livneh, B., Deems, J. S., Buma, B., Barsugli, J. J., Schneider, D., Molotch, N. P., et al. (2015). Catchment response to bark beetle outbreak and dust-on-snow in the Colorado Rocky Mountains. *Journal of Hydrology*, *523*, 196–210. https://doi.org/10.1016/j.jhydrol.2015.01.039

López-Moreno, J. I., Gascoin, S., Herrero, J., Sproles, E. A., Pons, M., Alonso-González, E., et al. (2017). Different sensitivities of snowpacks to warming in Mediterranean climate mountain areas. *Environmental Research Letters*, *12*, 074006. https://doi.org/10.1088/1748-9326/aa70cb

Louis, J.-F. (1979). A parametric model of vertical eddy fluxes in the atmosphere. *Boundary Layer Meteorology*, *17*, 187–202. https://doi.org/10.1007/bf00117978

MacDonald, M. K., Pomeroy, J. W., & Pietroniro, A. (2010). On the importance of sublimation to an alpine snow mass balance in the Canadian Rocky Mountains. *Hydrology and Earth System Sciences*, *14*, 1401–1415. https://doi.org/10.5194/hess-14-1401-2010

Mahat, V., & Tarboton, D. G. (2014). Representation of canopy snow interception, unloading and melt in a parsimonious snowmelt model. *Hydrological Processes*, *28*, 6320–6336. https://doi.org/10.1002/hyp.10116

Mahat, V., Tarboton, D. G., & Molotch, N. P. (2013). Testing above- and below-canopy representations of turbulent fluxes in an energy balance snowmelt model. *Water Resources Research*, *49*, 1107–1122. https://doi.org/10.1002/wrcr.20073

Marks, D., & Dozier, J. (1992). Climate and energy exchange at the snow surface in the alpine region of the Sierra-Nevada. 2. Snow cover energy-balance. *Water Resources Research*, *28*, 3043–3054. https://doi.org/10.1029/92WR01483

Marks, D., Reba, M., Pomeroy, J., Link, T., Winstral, A., Flerchinger, G., & Elder, K. (2008). Comparing simulated and measured sensible and latent heat fluxes over snow under a pine canopy to improve an energy balance snowmelt model. *Journal of Hydrometeorology*, *9*, 1506–1522. https://doi.org/10.1175/2008JHM874.1

McCabe, G. J., & Wolock, D. M. (2007). Warming may create substantial water supply shortages in the Colorado River basin. *Geophysical Research Letters*, *34*, L22708. https://doi.org/10.1029/2007GL031764

Meiman, J. R., & Grant, L. O. (1974). Snow-air interactions and management of mountain watershed snowpack (Completion Rep. Series 57, 36 pp.). Fort Collins, CO: Environmental Resources Center, Colorado State Univeristy.

Meromy, L., Molotch, N. P., Link, T. E., Fassnacht, S. R., & Rice, R. (2013). Subgrid variability of snow water equivalent at operational snow stations in the western USA. *Hydrological Processes*, *27*, 2383–2400. https://doi.org/10.1002/hyp.9355

Meyer, J. D. D., Jin, J. M., & Wang, S. Y. (2012). Systematic patterns of the inconsistency between snow water equivalent and accumulated precipitation as reported by the snowpack telemetry network. *Journal of Hydrometeorology*, *13*, 1970–1976. https://doi.org/10.1175/JHM-D-12-066.1

Mitchell, K. E., Lohmann, D., Houser, P. R., Wood, E. F., Schaake, J. C., Robock, A., et al. (2004). The multi-institution North American Land Data Assimilation System (NLDAS): Utilizing multiple GCIP products and partners in a continental distributed hydrological modeling system. *Journal of Geophysical Research*, *109*, D07S90. https://doi.org/10.1029/2003JD003823

Moeser, D., Mazzotti, G., Helbig, N., & Jonas, T. (2016). Representing spatial variability of forest snow: Implementation of a new interception model. *Water Resources Research*, *52*, 1208–1226. https://doi.org/10.1002/2015WR017961

Moeser, D., Stahli, M., & Jonas, T. (2015). Improved snow interception modeling using canopy parameters derived from airborne LiDAR data. *Water Resources Research*, *51*, 5041–5059. https://doi.org/10.1002/2014WR016724

Molotch, N. P., Blanken, P. D., Williams, M. W., Turnipseed, A. A., Monson, R. K., & Margulis, S. A. (2007). Estimating sublimation of intercepted and sub-canopy snow using eddy covariance systems. *Hydrological Processes*, *21*, 1567–1575. https://doi.org/10.1002/hyp.6719

Montesi, J., Elder, K., Schmidt, R. A., & Davis, R. E. (2004). Sublimation of intercepted snow within a subalpine forest canopy at two elevations. *Journal of Hydrometeorology*, *5*, 763–773. https://doi.org/10.1175/1525-7541(2004)005<0763:SOISWA>2.0.CO;2

Mote, P. W. (2006). Climate-driven variability and trends in mountain snowpack in western North America. *Journal of Climate*, *19*, 6209–6220. https://doi.org/10.1175/JCLI3971.1

Musselman, K. N., Clark, M. P., Liu, C. H., Ikeda, K., & Rasmussen, R. (2017). Slower snowmelt in a warmer world. *Nature Climate Change*, *7*, 214–219. https://doi.org/10.1038/nclimate3225

Musselman, K. N., Margulis, S. A., & Molotch, N. P. (2013). Estimation of solar direct beam transmittance of conifer canopies from airborne LiDAR. *Remote Sensing Environment*, *136*, 402–415. https://doi.org/10.1016/j.rse.2013.05.021

Musselman, K. N., Pomeroy, J. W., Essery, R. L. H., & Leroux, N. (2015). Impact of windflow calculations on simulations of alpine snow accumulation, redistribution and ablation. *Hydrological Processes*, *29*, 3983–3999. https://doi.org/10.1002/hyp.10595

Oke, T. R. (1987). *Boundary layer climates* (2nd ed., 435. pp.). New York, NY: Routledge Publishing.

Penn, C. A., Bearup, L. A., Maxwell, R. M., & Clow, D. W. (2016). Numerical experiments to explain multiscale hydrological responses to mountain pine beetle tree mortality in a headwater watershed. *Water Resources Research*, *52*, 3143–3161. https://doi.org/10.1002/2015WR018300

Pierce, D. W., Westerling, A. L., & Oyler, J. (2013). Future humidity trends over the western United States in the CMIP5 global climate models and variable infiltration capacity hydrological modeling system. *Hydrology and Earth System Sciences*, *17*, 1833–1850. https://doi.org/10.5194/hess-17-1833-2013

Pomeroy, J. W., & Essery, R. L. H. (1999). Turbulent fluxes during blowing snow: Field tests of model sublimation predictions. *Hydrological Processes*, *13*, 2963–2975. https://doi.org/10.1002/(SICI)1099-1085(19991230)13:18<2963::AID-HYP11>3.0.CO;2-9

Pomeroy, J. W., & Gray, D. M. (1995). Snow accumulation, relocation and management (National Hydrology Research Institute Science Rep. 7). Saskatchewan, Canada: Environment Canada, Saskatoon.

Pomeroy, J. W., Gray, D. M., Brown, T., Hedstrom, N. R., Quinton, W. L., Granger, R. J., & Carey, S. K. (2007). The cold regions hydrological model: A platform for basing process representation and model structure on physical evidence. *Hydrological Processes*, *21*, 2650–2667. https://doi.org/10.1002/hyp.6787

Pomeroy, J. W., & Male, D. H. (1992). Steady-state suspension of snow. *Journal of Hydrology*, *136*, 275–301. https://doi.org/10.1016/0022-1694(92)90015-N

Pomeroy, J. W., Parviainen, J., Hedstrom, N., & Gray, D. M. (1998). Coupled modelling of forest snow interception and sublimation. *Hydrological Processes*, *12*, 2317–2337. https://doi.org/10.1002/(SICI)1099-1085(199812)12:15<2317::AID-HYP799>3.0.CO;2-X

Potter, K. M., & Conkling, B. L. (2016). Forest health monitoring: National status, trends, and analysis 2015 (Gen. Tech. Rep. SRS-213). Asheville, NC: U.S. Department of Agriculture, Forest Service, Southern Research Station.

Prasad, R., Tarboton, D. G., Liston, G. E., Luce, C. H., & Seyfried, M. S. (2001). Testing a blowing snow model against distributed snow measurements at Upper Sheep Creek, Idaho, United States of America. *Water Resources Researach*, *37*, 1341–1356. https://doi.org/10.1029/2000WR900317

Price, A. G., & Dunne, T. (1976). Energy balance computations of snowmelt in a subarctic area. *Water Resources Research*, *12*, 686–694. https://doi.org/10.1029/WR012i004p00686

Pugh, E., & Gordon, E. (2013). A conceptual model of water yield effects from beetle-induced tree death in snow-dominated lodgepole pine forests. *Hydrological Processes*, *27*, 2048–2060. https://doi.org/10.1002/hyp.9312

Pugh, E., & Small, E. (2012). The impact of pine beetle infestation on snow accumulation and melt in the headwaters of the Colorado River. *Ecohydrology*, *5*, 467–477. https://doi.org/10.1002/eco.239

Raleigh, M. S., Lundquist, J. D., & Clark, M. P. (2015). Exploring the impact of forcing error characteristics on physically based snow simulations within a global sensitivity analysis framework. *Hydrology and Earth System Sciences*, *19*, 3153–3179. https://doi.org/10.5194/hess-19-3153-2015

Rasouli, K., Pomeroy, J. W., & Marks, D. G. (2015). Snowpack sensitivity to perturbed climate in a cool mid-latitude mountain catchment. *Hydrological Processes*, *29*, 3925–3940. https://doi.org/10.1002/hyp.10587

Rauscher, S. A., Pal, J. S., Diffenbaugh, N. S., & Benedetti, M. M. (2008). Future changes in snowmelt-driven runoff timing over the western US. *Geophysical Research Letters*, *35*, L16703. https://doi.org/10.1029/2008GL034424

Reba, M. L., Link, T. E., Marks, D., & Pomeroy, J. (2009). An assessment of corrections for eddy covariance measured turbulent fluxes over snow in mountain environments. *Water Resources Research*, *45*, W00D38. https://doi.org/10.1029/2008WR007045

Reba, M. L., Pomeroy, J., Marks, D., & Link, T. E. (2012). Estimating surface sublimation losses from snowpacks in a mountain catchment using eddy covariance and turbulent transfer calculations. *Hydrological Processes*, *26*, 3699–3711. https://doi.org/10.1002/hyp.8372

Richer, E. E., Kampf, S. K., Fassnacht, S. R., & Moore, C. C. (2013). Spatiotemporal index for analyzing controls on snow climatology: Application in the Colorado Front Range. *Physical Geography*, *34*, 85–107. https://doi.org/10.1080/02723646.2013.787578

Senay, G. B., Bohms, S., Singh, R. K., Gowda, P. H., Velpuri, N. M., Alemu, H., & Verdin, J. P. (2013). Operational evapotranspiration mapping using remote sensing and weather datasets: A new parameterization for the SSEB approach. *Journal of American Water Resources Association*, *49*, 577–591. https://doi.org/10.1111/jawr.12057

Sexstone, G. A., Clow, D. W., Stannard, D. I., & Fassnacht, S. R. (2016). Comparison of methods for quantifying surface sublimation over seasonally snow-covered terrain. *Hydrological Processes*, *30*, 3373–3389. https://doi.org/10.1002/hyp.10864

Sogachev, A., Rannik, U., & Vesala, T. (2004). Flux footprints over complex terrain covered by heterogeneous forest. *Agricultural and Forest Meteorology*, *127*, 143–158. https://doi.org/10.1016/j.agrformet.2004.07.010

Solomon, S., D. Qin, M. Manning, M. Marquis, K. Averyt, M. M. B. Tignor, et al. (Eds.). (2007). *Climate change 2007: The physical science basis, contribution of working group I to the fourth assessment report of the intergovernmental panel on climate change*. Cambridge, UK: Cambridge University Press.

Sproles, E. A., Nolin, A. W., Rittger, K., & Painter, T. H. (2013). Climate change impacts on maritime mountain snowpack in the Oregon Cascades. *Hydrology and Earth System Sciences*, *17*, 2581–2597. https://doi.org/10.5194/hess-17-2581-2013

Stewart, I. T. (2009). Changes in snowpack and snowmelt runoff for key mountain regions. *Hydrological Processes*, *23*, 78–94. https://doi.org/10.1002/hyp.7128

Stocker T. F., D. Qin, G.-K. Plattner, M. Tignor, S. K. Allen, J. Boschung, et al. (Eds.). (2013). *Climate change 2013: The physical science basis, contribution of working group I to the fifth assessment report of the intergovernmental panel on climate change*. Cambridge, UK: Cambridge University Press.

Strasser, U., Bernhardt, M., Weber, M., Liston, G. E., & Mauser, W. (2008). Is snow sublimation important in the alpine water balance? *The Cryosphere*, *2*, 53–66.

Svoma, B. M. (2017). Canopy effects on snow sublimation from a central Arizona Basin. *Journal of Geophysical Research: Atmospheres*, *122*, 20–46. https://doi.org/10.1002/2016JD025184

Taylor, J. R. (1997). *An introduction to error analysis* (2nd ed., 327. pp.). Sausalito, CA: University Science Books.

Trujillo, E., & Molotch, N. P. (2014). Snowpack regimes of the Western United States. *Water Resources Research*, *50*, 5611–5623. https://doi.org/10.1002/2013WR014753

Turnipseed, A. A., Blanken, P. D., Anderson, D. E., & Monson, R. K. (2002). Energy budget above a high-elevation subalpine forest in complex topography. *Agricultural and Forest Meteorology*, *110*, 177–201. https://doi.org/10.1016/S0168-1923(01)00290-8